Statistical Evaluation

An unpaired Student t test was used for the biodistribution experiments. One-way ANOVA followed by the Dunnett post hoc test compared with the untreated group was used for experiments on allodynia measurements, comparisons of tumor growth, WBC counts, and platelet counts. Results were considered statistically significant at $P < 0.05$.

RESULTS

Biodistribution in Normal Rats

The biodistributions of ^{186}Re-MAG3-HBP and ^{186}Re-HEDP in normal rats are presented in Table 1. Both compounds showed a rapid accumulation and long residence in the bone. The uptake of ^{186}Re-MAG3-HBP in the bone was significantly higher than that of ^{186}Re-HEDP.

Imaging

The planar images at 24 h after injection of ^{186}Re-MAG3-HBP and ^{186}Re-HEDP showed a marked accumulation of radioactivity surrounding the site of inoculation of the tumor cells (Fig. 2). In tissues other than bone, no significant accumulation of radioactivity was observed, a reflection of the results of the biodistribution experiments.

Tumoral bone-to-normal bone ratios of ^{186}Re-MAG3-HBP and ^{186}Re-HEDP were 3.54 ± 0.60 and 2.90 ± 0.97, respectively (mean ± SD). This difference was not statistically significant.

TABLE 1
Biodistribution of ^{186}Re-MAG3-HBP and ^{186}Re-HEDP in Rats

Tissue	Time after administration		
	10 min	3 h	24 h
	^{186}Re-MAG3-HBP (%ID/g tissue)		
Blood	0.831 ± 0.134*	0.015 ± 0.008†	0.003 ± 0.000†
Liver	0.213 ± 0.031*	0.063 ± 0.025	0.051 ± 0.009†
Kidney	1.551 ± 0.115	0.539 ± 0.187*	0.473 ± 0.074
Intestine	0.153 ± 0.015*	0.235 ± 0.173	0.151 ± 0.081
Spleen	0.180 ± 0.018*	0.030 ± 0.009	0.027 ± 0.005*
Pancreas	0.196 ± 0.024	0.013 ± 0.003*	0.008 ± 0.002
Lung	0.566 ± 0.059†	0.040 ± 0.009*	0.037 ± 0.031
Stomach‡	0.525 ± 0.198	0.302 ± 0.134*	0.152 ± 0.176*
Femur	2.129 ± 0.142*	3.943 ± 0.270†	4.097 ± 0.181†
Muscle	0.129 ± 0.028	0.014 ± 0.009	0.004 ± 0.001
	^{186}Re-HEDP (%ID/g tissue)		
Blood	0.572 ± 0.103	0.074 ± 0.025	0.025 ± 0.006
Liver	0.162 ± 0.020	0.035 ± 0.005	0.025 ± 0.005
Kidney	1.807 ± 0.613	0.859 ± 0.162	0.386 ± 0.115
Intestine	0.126 ± 0.012	0.074 ± 0.039	0.082 ± 0.039
Spleen	0.133 ± 0.019	0.032 ± 0.005	0.020 ± 0.003
Pancreas	0.164 ± 0.021	0.019 ± 0.003	0.013 ± 0.004
Lung	0.414 ± 0.049	0.067 ± 0.014	0.032 ± 0.013
Stomach‡	0.710 ± 0.323	0.729 ± 0.284	0.764 ± 0.440
Femur	1.586 ± 0.365	1.913 ± 0.272	1.798 ± 0.621
Muscle	0.117 ± 0.024	0.011 ± 0.005	0.005 ± 0.003

*$P < 0.05$ vs. ^{186}Re-HEDP.
†$P < 0.01$ vs. ^{186}Re-HEDP.
‡Data are expressed as percentage injected dose (%ID).
Data are expressed as mean ± SD for 4 animals.

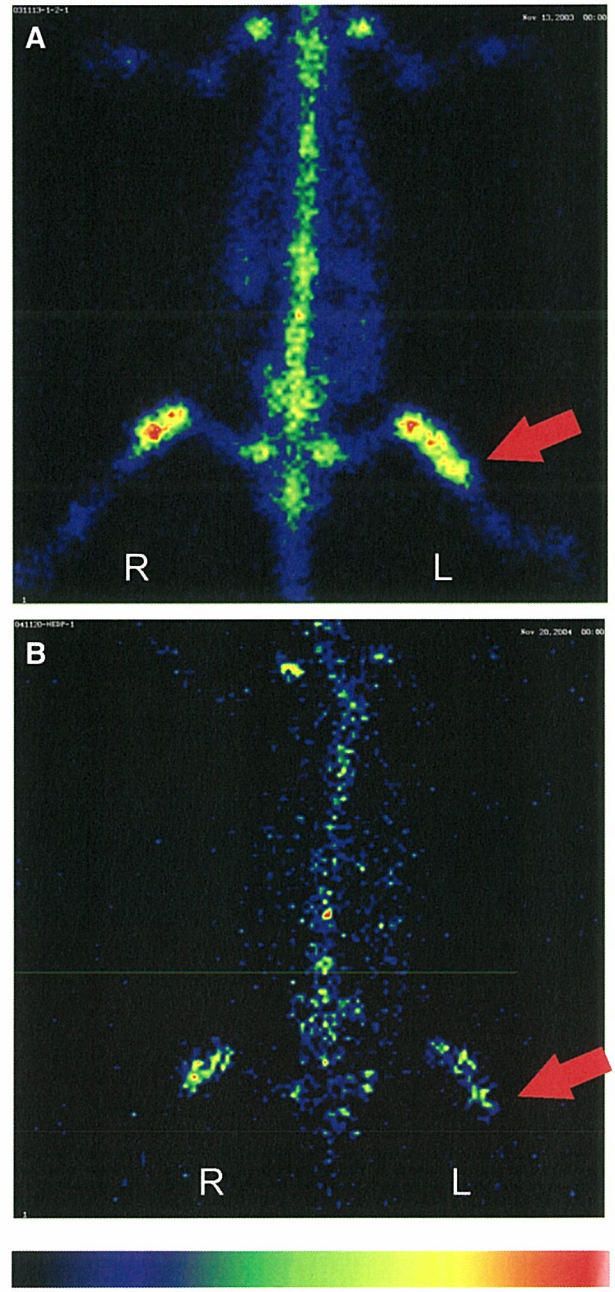

FIGURE 2. Planar images at 24 h after intravenous injection of ^{186}Re-MAG3-HBP (222 MBq/kg) (A) and ^{186}Re-HEDP (55.5 MBq/kg) (B). Arrows indicate the site where tumor cells were injected.

Therapeutic Effects

The volume of the tumors as a function of time is shown in Figure 3. As can be seen, the MRMT-1 tumor cells proliferated exponentially after a palpable tumor developed in the left tibia. In rats treated with ^{186}Re-HEDP at a dose of 55.5 MBq/kg, tumor growth was comparable with that of untreated rats. In

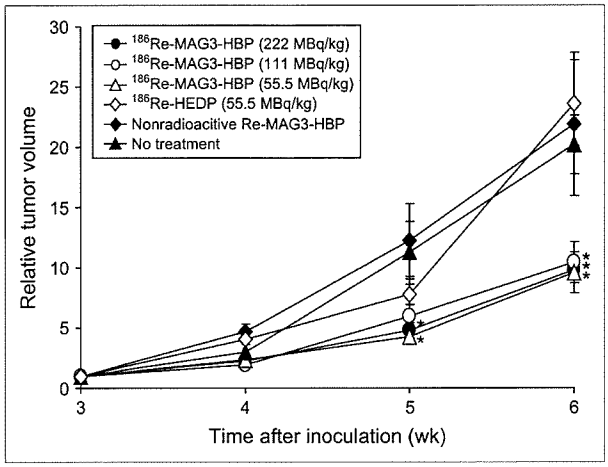

FIGURE 3. Curves show inhibition of growth of MRMT-1 tumor cells on therapy. Data are expressed as tumor volume relative to that on day of treatment (mean ± SEM for 5–7 rats). Significance was determined using 1-way ANOVA followed by the Dunnett post hoc test (*$P < 0.05$ vs. no treatment).

contrast, when ^{186}Re-MAG3-HBP was administered at the same dose as ^{186}Re-HEDP, tumor growth was significantly inhibited compared with that of the untreated group.

Palliative effects determined by the von Frey filament test are shown in Figure 4. A larger value indicates more intense pain on the cancer-bearing side. In untreated rats, the enhanced withdrawal response to mechanical stimulation with von Frey filaments caused by cancer-induced bone pain was elevated. Both ^{186}Re-MAG3-HBP and ^{186}Re-HEDP attenuated this mechanical allodynia but ^{186}Re-MAG3-HBP tended to be more effective.

The injected dose of ^{186}Re-MAG3-HBP ranged from 55.5 to 222 MBq/kg, and the therapeutic effects were assessed. Consequently, it was found that the inhibition of tumor growth and the response in terms of the palliation of pain were not correlated with the treatment dose (Figs. 3 and 4).

Moreover, when nonradioactive Re-MAG3-HBP was administered, tumor growth and the withdrawal response were not significant compared with those in untreated rats (Figs. 3 and 4).

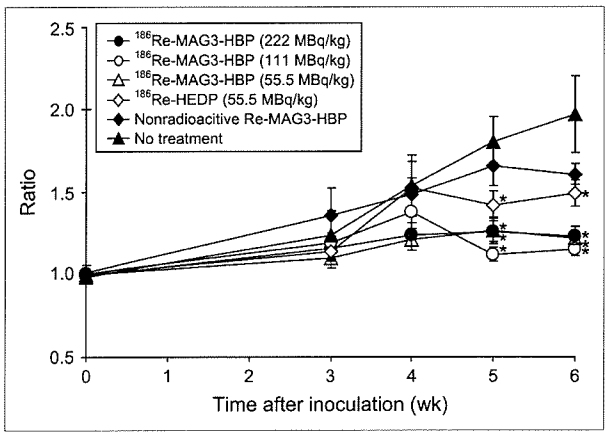

FIGURE 4. Effects of radiopharmaceuticals on bone cancer pain. Data are expressed as ratio of right (contralateral) withdrawal paw threshold values to left (ipsilateral) values (mean ± SEM for 5–7 rats). Significance was determined using 1-way ANOVA followed by the Dunnett post hoc test (*$P < 0.05$ vs. no treatment).

Myelotoxicity

When ^{186}Re-MAG3-HBP or ^{186}Re-HEDP was administered, WBC and platelet counts tended to decrease at 1 and 2 wk after treatment, especially in the case of high-dose treatment with ^{186}Re-MAG3-HBP. However, the decreases were not critical, and these counts were recovered within 3 wk after the injection (Fig. 5).

DISCUSSION

In general, the use of an appropriate animal model is important for the evaluation of the therapeutic effects of

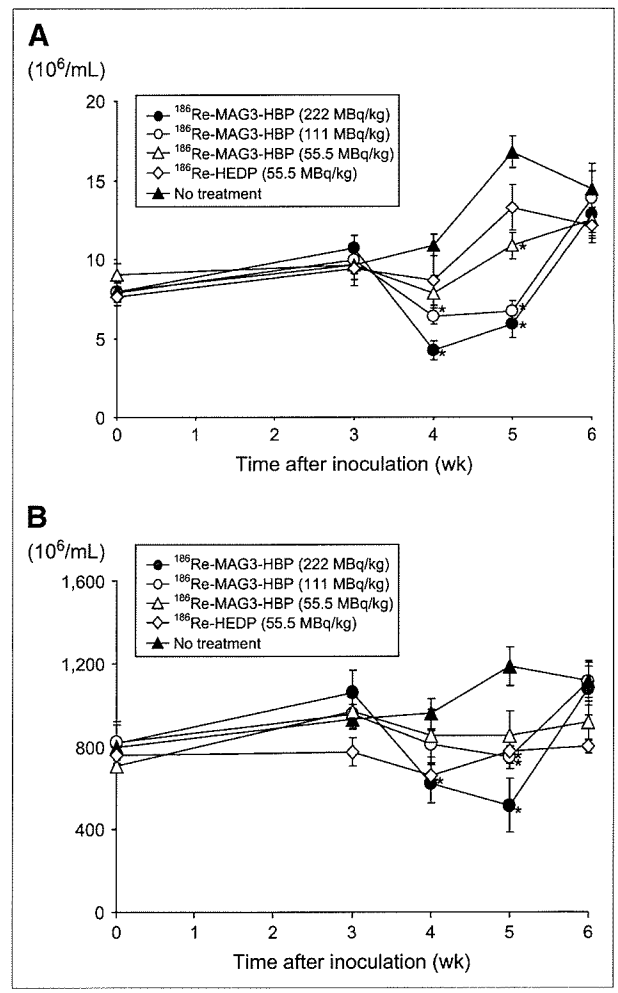

FIGURE 5. WBC (A) and thrombocyte (B) counts in rat model of bone metastasis under treatment. Data are presented as mean ± SEM for 5–7 rats. Significance was determined using 1-way ANOVA followed by the Dunnett post hoc test (*$P < 0.05$ vs. no treatment).

pharmaceuticals. For the evaluation of therapeutic effects of radiopharmaceuticals on metastatic bone tumors, a heart injection model has often been used (*19,20*). This model involves the direct introduction of tumor cells into the arterial circulation through the left ventricle of the heart in nude mice or nude rats (*21,22*). It is useful for the evaluation of survival (*19,20*) but is unsuitable for the evaluation of palliation of metastatic bone pain because it has multiple lesion sites. Furthermore, to our knowledge, there has been no report on an appropriate animal model for the evaluation of the palliating effects of radiopharmaceuticals on metastatic bone pain. However, intrabone injection models have recently been developed as a model of bone tumor pain (*16,23,24*). In this study, we used one of these models, the intratibial injection model, for the following reasons: (a) the radiologic, histologic, and behavioral characteristics resemble those of patients with bone metastases (*5,16,25*); (b) it is possible to equalize the position of single lesions in all experimental animals; (c) bone cancer pain can be quantitatively evaluated using a von Frey filament test; and (d) the surgery is simple and barely invasive.

The von Frey filament test is a way to examine withdrawal responses for mechanical stimuli to the hind paw of rats using various different von Frey filaments and has frequently been used for evaluating mechanical allodynia, especially in a neuropathic pain model (*17,18*). Recently, the test has also been used in a metastasis model (*16,25*). Bone cancer pain can be intermittent, but it progresses rapidly into continuous pain that is exacerbated by episodes of breakthrough pain. Once this chronic pain is established, the condition of the patient deteriorates further when mechanical allodynia develops. Mechanical allodynia occurs when normally nonpainful activity or stimulation is perceived as painful. For example, coughing, turning in bed, or gentle limb movement can cause intense pain (*26*). Accordingly, evaluating mechanical allodynia as an index of pain in the model is meaningful.

Moreover, it has been reported that levels of osteoblastic/osteoclastic activity were high in areas close to the tumor because the MRMT-1 cells used in this model produce a mixed type of bone lesion (*16*). Most bone-seeking radiopharmaceuticals, including ^{186}Re-MAG3-HBP, accumulate at sites with strong osteoblastic activity. Accordingly, we assumed that this model might be adequate to evaluate the therapeutic effects of bone-seeking radiopharmaceuticals.

The main finding of this study is that a single treatment with ^{186}Re-MAG3-HBP, a ^{186}Re-complex–conjugated bisphosphonate, achieved significant inhibition of tumor growth and palliation of pain in a rat model of bone metastasis (Figs. 3 and 4). ^{186}Re-HEDP palliated the pain but did not inhibit tumor growth. Although the mechanism of the palliation of bone cancer pain by radiotherapy remains unclear, a radiation-induced reduction of tumor size has been considered one of the causes (*27,28*). However, empiric data from experiments with external irradiation indicate that the absorbed dose required to achieve pain relief is significantly lower than that necessary to achieve a tumoricidal effect (*29–31*). Because ^{186}Re-MAG3-HBP showed much greater accumulation in normal bone than did ^{186}Re-HEDP in biodistribution experiments with normal rats and because there was no significant difference between the tumoral bone-to-normal bone ratios of ^{186}Re-MAG3-HBP and ^{186}Re-HEDP in the bone metastasis model, the difference in the inhibition of tumor growth between the 2 radiopharmaceuticals could be attributed to the difference in accumulation at the site of bone metastasis. Furthermore, the inhibition of tumor growth should result in a more effective palliation than that achieved with ^{186}Re-HEDP.

The pain-relieving effect of ^{186}Re-MAG3-HBP was not dependent on dose (Fig. 4). This result is consistent with the clinical observations in breast cancer patients that the response rate in terms of pain reduction was not correlated with the dose of ^{186}Re-HEDP (*10*). Contrary to expectation, raising the dose of ^{186}Re-MAG3-HBP did not potentiate the inhibition of tumor growth. Although the reason for this is unclear, no serious toxic effects were observed on high-dose treatment. Therefore, it is necessary to examine the effect of increasing the dose of ^{186}Re-MAG3-HBP on tumor growth using other models.

Bisphosphonates have been used primarily to treat hypercalcemia (from excess bone resorption) and, more recently, cancer-induced bone pain (*32*). Recent reports indicate that the regular use of bisphosphonates for metastatic bone disease prevents skeletal-related events, reduces bone pain, and improves the patient's quality of life (*32,33*). Briefly, the mechanism of action includes induction of the apoptosis of osteoclasts, inhibition of the proliferation of cancer cells, and reduction in the production of cytokine and secretion of metalloproteinase. Walker et al. reported that zoledronic acid, a bisphosphonate, was a useful antinociceptive agent in a rat model of metastatic cancer pain (*25*). These findings raise the possibility that the therapeutic effect of ^{186}Re-MAG3-HBP is attributable not to the β-particles of ^{186}Re but, rather, to the bisphosphonate structure of ^{186}Re-MAG3-HBP. To test this possibility, we treated rats with nonradioactive Re-MAG3-HBP at the same dose as ^{186}Re-MAG3-HBP. In nonradioactive Re-MAG3-HBP–treated rats, tumor growth and the withdrawal response were comparable with those in untreated rats (Figs. 3 and 4). Accordingly, the therapeutic effect of ^{186}Re-MAG3-HBP can be attributed to the β-particles of ^{186}Re.

CONCLUSION

^{186}Re-MAG3-HBP accumulated at the site where tumor cells were injected in a rat model of bone cancer and significantly inhibited tumor growth and attenuated the allodynia induced by bone cancer without having critical myelosuppressive side effects. These results indicate that ^{186}Re-MAG3-HBP could be useful as a therapeutic agent for the palliation of metastatic bone pain.

ACKNOWLEDGMENTS

This work was supported in part by a Grant-in-Aid for Scientific Research on Priority Areas from the Ministry of

Education, Culture, Sports, Science and Technology of Japan and by a research grant from the Sagawa Foundation for the Promotion of Cancer Research.

REFERENCES

1. Yoneda T, Sasaki A, Mundy GR. Osteolytic bone metastasis in breast cancer. *Breast Cancer Res Treat.* 1994;32:73–84.
2. Coleman RE. Skeletal complications of malignancy. *Cancer.* 1997;80:1588–1594.
3. Portenoy RK, Lesage P. Management of cancer pain. *Lancet.* 1999;353:1695–1700.
4. Portenoy RK, Payne D, Jacobsen P. Breakthrough pain: characteristics and impact in patients with cancer pain. *Pain.* 1999;81:129–134.
5. Mercadante S. Malignant bone pain: pathophysiology and treatment. *Pain.* 1997; 69:1–18.
6. Arcangeli G, Giovinazzo G, Saracino B, D'Angelo L, Giannarelli D, Micheli A. Radiation therapy in the management of symptomatic bone metastases: the effect of total dose and histology on pain relief and response duration. *Int J Radiat Oncol Biol Phys.* 1998;42:1119–1126.
7. Lewington VJ. Bone-seeking radionuclides for therapy. *J Nucl Med.* 2005; 46(suppl 1):38S–47S.
8. Finlay IG, Mason MD, Shelley M. Radioisotopes for the palliation of metastatic bone cancer: a systematic review. *Lancet Oncol.* 2005;6:392–400.
9. Limouris GS, Shukla SK, Condi-Paphiti A, et al. Palliative therapy using rhenium-186-HEDP in painful breast osseous metastases. *Anticancer Res.* 1997; 17:1767–1772.
10. Lam MG, de Klerk JM, van Rijk PP. ^{186}Re-HEDP for metastatic bone pain in breast cancer patients. *Eur J Nucl Med Mol Imaging.* 2004;31(suppl 1):S162–S170.
11. de Klerk JM, van Dijk A, van het Schip AD, Zonnenberg BA, van Rijk PP. Pharmacokinetics of rhenium-186 after administration of rhenium-186-HEDP to patients with bone metastases. *J Nucl Med.* 1992;33:646–651.
12. De Winter F, Brans B, Van De Wiele C, Dierckx RA. Visualization of the stomach on rhenium-186 HEDP imaging after therapy for metastasized prostate carcinoma. *Clin Nucl Med.* 1999;24:898–899.
13. Ogawa K, Mukai T, Arano Y, et al. Design of a radiopharmaceutical for the palliation of painful bone metastases: rhenium-186-labeled bisphosphonate derivative. *J Labelled Compds Radiopharm.* 2004;47:753–761.
14. Ogawa K, Mukai T, Arano Y, et al. Rhemium-186-monoaminemonoamidedithiols conjugated bisphosphonate derivatives for bone pain palliation. *Nucl Med Biol.* 2006;33:513–520.
15. Ogawa K, Mukai T, Arano Y, et al. Development of a rhenium-186-labeled MAG3-conjugated bisphosphonate for the palliation of metastatic bone pain based on the concept of bifunctional radiopharmaceuticals. *Bioconjug Chem.* 2005;16:751–757.
16. Medhurst SJ, Walker K, Bowes M, et al. A rat model of bone cancer pain. *Pain.* 2002;96:129–140.
17. Kim SH, Chung JM. An experimental model for peripheral neuropathy produced by segmental spinal nerve ligation in the rat. *Pain.* 1992;50:355–363.
18. Okada M, Nakagawa T, Minami M, Satoh M. Analgesic effects of intrathecal administration of P2Y nucleotide receptor agonists UTP and UDP in normal and neuropathic pain model rats. *J Pharmacol Exp Ther.* 2002;303:66–73.
19. Henriksen G, Breistol K, Bruland O, Fodstad O, Larsen R. Significant antitumor effect from bone-seeking, alpha-particle-emitting ^{223}Ra demonstrated in an experimental skeletal metastases model. *Cancer Res.* 2002;62:3120–3125.
20. Arstad E, Hoff P, Skattebol L, Skretting A, Breistol K. Studies on the synthesis and biological properties of non-carrier-added [^{125}I and ^{131}I]-labeled arylalkylidenebisphosphonates: potent bone-seekers for diagnosis and therapy of malignant osseous lesions. *J Med Chem.* 2003;46:3021–3032.
21. Engebraaten O, Fodstad O. Site-specific experimental metastasis patterns of two human breast cancer cell lines in nude rats. *Int J Cancer.* 1999;82:219–225.
22. Yoneda T, Michigami T, Yi B, Williams PJ, Niewolna M, Hiraga T. Actions of bisphosphonate on bone metastasis in animal models of breast carcinoma. *Cancer.* 2000;88:2979–2988.
23. Schwei MJ, Honore P, Rogers SD, et al. Neurochemical and cellular reorganization of the spinal cord in a murine model of bone cancer pain. *J Neurosci.* 1999;19:10886–10897.
24. Honore P, Luger NM, Sabino MA, et al. Osteoprotegerin blocks bone cancer-induced skeletal destruction, skeletal pain and pain-related neurochemical reorganization of the spinal cord. *Nat Med.* 2000;6:521–528.
25. Walker K, Medhurst SJ, Kidd BL, et al. Disease modifying and anti-nociceptive effects of the bisphosphonate, zoledronic acid in a model of bone cancer pain. *Pain.* 2002;100:219–229.
26. Clohisy DR, Mantyh PW. Bone cancer pain. *Cancer.* 2003;97:866–873.
27. Goblirsch M, Mathews W, Lynch C, et al. Radiation treatment decreases bone cancer pain, osteolysis and tumor size. *Radiat Res.* 2004;161:228–234.
28. Bone Pain Trial Working Party. 8 Gy single fraction radiotherapy for the treatment of metastatic skeletal pain: randomised comparison with a multifraction schedule over 12 months of patient follow-up. *Radiother Oncol.* 1999;52:111–121.
29. Hoskin PJ. Bisphosphonates and radiation therapy for palliation of metastatic bone disease. *Cancer Treat Rev.* 2003;29:321–327.
30. Vakaet LA, Boterberg T. Pain control by ionizing radiation of bone metastasis. *Int J Dev Biol.* 2004;48:599–606.
31. Vit JP, Ohara PT, Tien DA, et al. The analgesic effect of low dose focal irradiation in a mouse model of bone cancer is associated with spinal changes in neuro-mediators of nociception. *Pain.* 2006;120:188–201.
32. Mystakidou K, Katsouda E, Stathopoulou E, Vlahos L. Approaches to managing bone metastases from breast cancer: the role of bisphosphonates. *Cancer Treat Rev.* 2005;31:303–311.
33. Body JJ. Bisphosphonates for malignancy-related bone disease: current status, future developments. *Support Care Cancer.* 2006;14:408–418.

Development of a Novel ^{99m}Tc-Chelate–Conjugated Bisphosphonate with High Affinity for Bone as a Bone Scintigraphic Agent

Kazuma Ogawa[1,2], Takahiro Mukai[1,3], Yasuyuki Inoue[1], Masahiro Ono[1], and Hideo Saji[1]

[1]Department of Patho-Functional Bioanalysis, Graduate School of Pharmaceutical Sciences, Kyoto University, Kyoto, Japan; [2]Division of Tracer Kinetics, Advanced Science Research Center, Kanazawa University, Kanazawa, Japan; and [3]Department of Biomolecular Recognition Chemistry, Graduate School of Pharmaceutical Sciences, Kyushu University, Fukuoka, Japan

In bone scintigraphy using ^{99m}Tc with methylenediphosphonate (^{99m}Tc-MDP) and hydroxymethylenediphosphonate (^{99m}Tc-HMDP), it takes 2–6 h after an injection before imaging can start. This interval could be shortened with a new radiopharmaceutical with higher affinity for bone. Here, based on the concept of bifunctional radiopharmaceuticals, we designed a ^{99m}Tc-mercaptoacetylglycylglycylglycine (MAG3)-conjugated hydroxy-bisphosphonate (HBP) (^{99m}Tc-MAG3-HBP) and a ^{99m}Tc-6-hydrazinopyridine-3-carboxylic acid (HYNIC)-conjugated hydroxy-bisphosphonate (^{99m}Tc-HYNIC-HBP). **Methods:** ^{99m}Tc-MAG3-HBP was prepared by complexation of MAG3-HBP with ^{99m}Tc using $SnCl_2$ as a reductant. The precursor of ^{99m}Tc-HYNIC-HBP, HYNIC-HBP, was obtained by deprotection of the Boc group after the coupling of Boc-HYNIC to a bisphosphonate derivative. ^{99m}Tc-HYNIC-HBP was prepared by a 1-pot reaction of HYNIC-HBP with $^{99m}TcO_4^-$, tricine, and 3-acetylpyridine in the presence of $SnCl_2$. Affinity for bone was evaluated in vitro by hydroxyapatite-binding assays for ^{99m}Tc-HMDP, ^{99m}Tc-MAG3-HBP, and ^{99m}Tc-HYNIC-HBP. Biodistribution experiments for the 3 ^{99m}Tc-labeled compounds were performed on normal rats. **Results:** ^{99m}Tc-MAG3-HBP and ^{99m}Tc-HYNIC-HBP were each prepared with a radiochemical purity of >95%. In the in vitro binding assay, ^{99m}Tc-MAG3-HBP and ^{99m}Tc-HYNIC-HBP had greater affinity for hydroxyapatite than ^{99m}Tc-HMDP. In the biodistribution experiments, ^{99m}Tc-MAG3-HBP and ^{99m}Tc-HYNIC-HBP had higher levels of radioactivity in bone than ^{99m}Tc-HMDP. ^{99m}Tc-MAG3-HBP was cleared from the blood slower than ^{99m}Tc-HMDP, whereas there was no significant difference in clearance between ^{99m}Tc-HYNIC-HBP and ^{99m}Tc-HMDP. Consequently, ^{99m}Tc-HYNIC-HBP showed a higher bone-to-blood ratio than ^{99m}Tc-HMDP. **Conclusion:** We developed a novel ^{99m}Tc-chelate–conjugated bisphosphonate with high affinity for bone and rapid clearance from blood, based on the concept of bifunctional radiopharmaceuticals. The present findings indicate that ^{99m}Tc-HYNIC-HBP holds great potential for bone scintigraphy.

Key Words: bone scintigraphy; bisphosphonate; ^{99m}Tc; MAG3; HYNIC

J Nucl Med 2006; 47:2042–2047

Over the last quarter of a century, complexes of ^{99m}Tc with methylenediphosphonate (^{99m}Tc-MDP) and hydroxymethylenediphosphonate (^{99m}Tc-HMDP) have been widely used as radiopharmaceuticals for bone scintigraphy in cases of metastatic bone disease, Paget's disease, fractures in osteoporosis, and so forth (*1–4*). With these ^{99m}Tc-labeled bisphosphonates, however, an interval of 2–6 h is needed between injection and bone imaging (*3*). Shorting this interval would lessen the burden on patients in terms of the total length of the examination and the dose of radiation absorbed. To enable imaging at an earlier time after injection, a radiopharmaceutical with higher affinity for bone is required.

Bisphosphonate analogs accumulate in bone because their phosphonate groups bind to the Ca^{2+} of hydroxyapatite crystals (*5*). In the case of ^{99m}Tc-MDP and ^{99m}Tc-HMDP, the phosphonate groups coordinate with technetium (*6*), which might decrease the inherent accumulation of MDP and HMDP in bone. Thus, we hypothesized that bone affinity of ^{99m}Tc-labeled bisphosphonate would be increased by the design of a bisphosphonate in which the phosphonate groups do not coordinate with technetium, and we attempted to design a ^{99m}Tc-chelate–conjugated bisphosphonate based on the concept of bifunctional radiopharmaceuticals (Fig. 1). In this study, mercaptoacetylglycylglycylglycine (MAG3) and 6-hydrazinopyridine-3-carboxylic acid (HYNIC) were chosen as chelating sites because they have been widely used for ^{99m}Tc labeling of proteins and peptides (*7–11*) and conjugated to 4-amino-1-hydroxybutylidene-1,1-bisphosphonate. Then, ^{99m}Tc-[[[(4-hydroxy-4,4-diphosphonobutyl)carbamoylmethyl]carbamoylmethyl]carbamoylmethyl]carbamoylmethanethiolate (^{99m}Tc-MAG3-HBP; Fig. 1A) and [^{99m}Tc][[4-[(6-hydrazinopyridine-3-carbonyl)amino]-1-hydroxy-1-phosphonobutyl]phosphonic acid](tricine)(3-acetylpyridine) (^{99m}Tc-HYNIC-HBP; Fig. 1B) were

Received May 9, 2006; Revision accepted Sep. 6, 2006.

For correspondence or reprints contact: Hideo Saji, PhD, Department of Patho-Functional Bioanalysis, Graduate School of Pharmaceutical Sciences, Kyoto University, Sakyo-ku, Kyoto 606-8501, Japan.
E-mail: hsaji@pharm.kyoto-u.ac.jp

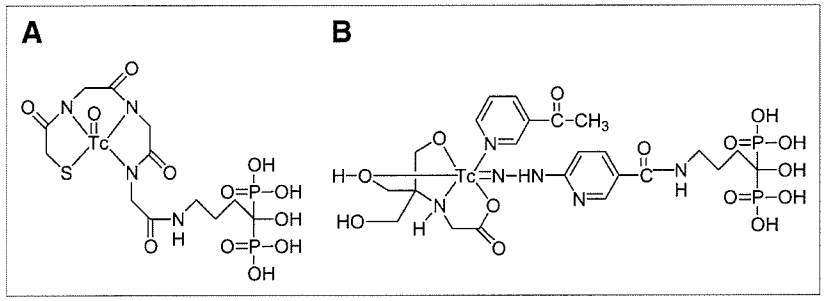

FIGURE 1. Chemical structures of ^{99m}Tc-MAG3-HBP (A) and ^{99m}Tc-HYNIC-HBP (B).

prepared by coordination with ^{99m}Tc, and their properties in vitro and in vivo were compared with these of ^{99m}Tc-HMDP.

MATERIALS AND METHODS

Materials

Proton nuclear magnetic resonance (^{1}H NMR) spectra were recorded on a Bruker AC-200 spectrometer (JEOL Ltd.), and the chemical shifts were reported in parts per million downfield from an internal 3-(trimethylsilyl)propionic-2,2,3,3-d_4 acid sodium salt standard. Electrospray ionization mass spectra (ESI-MS) were obtained with a LCMS-QP8000α (Shimadzu). Thin-layer chromatographic analyses were performed with silica plates (Silica gel 60; Merck KGaA) with acetone as a developing solvent. ^{99m}Tc-Pertechnetate ($^{99m}TcO_4^-$) was eluted in a saline solution on a daily basis from generators (Daiichi Radioisotope Laboratories, Ltd.). ^{99m}Tc-HMDP was prepared by reconstitution with a conventional HMDP labeling kit (Nihon Medi-Physics Co., Ltd.) with a $^{99m}TcO_4^-$ solution. Other reagents were of reagent grade and were used as received.

Preparation of ^{99m}Tc-MAG3-HBP

The precursor of ^{99m}Tc-MAG3-HBP, [1-hydroxy-1-phosphono-4-[2-[2-[2-(2-tritylmercaptoacetylamino)-acetylamino]acetylamino] acetylamino]butyl]phosphonic acid (Tr-MAG3-HBP) was synthesized according to procedures described previously (*12*). The trityl group of Tr-MAG3-HBP (0.1 mg) was dissolved in 190 μL of trifluoroacetic acid (TFA) and 10 μL of triethylsilane. After removal of the solvent under a stream of N_2, 80 μL of 0.1 mol/L borate buffer (pH 9.5) were added to the residue. Next, 3 μL of $SnCl_2 \cdot 2H_2O$ solution in 0.1 mol/L citrate buffer (pH 5.0) (1 mg/mL) and 200 μL of $^{99m}TcO_4^-$ solution were added, and the reaction mixture was vigorously stirred and allowed to react at 95°C for 1 h. ^{99m}Tc-MAG3-HBP was purified by reversed-phase high-performance liquid chromatography (RP-HPLC) performed with a Cosmosil 5C_{18}-AR-300 column (4.6 × 150 mm; Nacalai Tesque) at a flow rate of 1 mL/min with a mixture of 0.2 mol/L phosphate buffer (pH 6.0) and ethanol (90:10) containing 10 mmol/L tetrabutylammonium hydroxide.

Preparation of [[[[(4-Hydroxy-4,4-Diphosphonobutyl) Carbamoylmethyl]Carbamoylmethyl]Carbamoylmethyl] Carbamoylmethanethiolate] Oxorhenium(V) (Re-MAG3-HBP)

Re-MAG3-HBP was synthesized according to procedures described previously (*12*). ESI-MS calculated for $C_{12}H_{20}N_4O_{12}P_2{}^{187}ReS$ (M- H)$^-$: m/z 692. Found: 692 $C_{12}H_{20}N_4O_{12}P_2{}^{185}ReS$ (M- H)$^-$: m/z 690. Found: 690.

Preparation of ^{99m}Tc-HYNIC-HBP

2,3,5,6-Tetrafluorophenyl 6-(tert-butoxycarbonyl)-hydrazinopyridine-3-carboxylate (Boc-HYNIC-TFP) and 4-amino-1-hydroxybutylidene-1,1-bisphosphonate were synthesized according to procedures described preciously (*12,13*). 4-Amino-1-hydroxybutylidene-1,1-bisphosphonate (10.3 mg, 41.3 μmol) was suspended in 1.33 mL of distilled water, and triethylamine (25.1 mg, 248 μmol) was added to the suspension. After a few seconds of stirring at room temperature, Boc-HYNIC-TFP (17.8 mg, 44.4 μmol) dissolved in 1.33 mL of acetonitrile was added. The reaction mixture was stirred for 3 h at room temperature. RP-HPLC was performed with a Hydrosphere 5C18 column (20 × 150 mm; YMC Co., Ltd) at a flow rate of 16 mL/min with a mixture of water, acetonitrile, and formic acid (90:10:1). Chromatograms were obtained by monitoring the ultraviolet (UV) adsorption at a wavelength of 254 nm. The fraction containing [4-[[6-(tert-butoxycarbonyl)-hydrazinopyridine-3-carbonyl]amino]-1-hydroxy-1-phosphonobutyl]phosphonic acid (Boc-HYNIC-HBP) was identified by mass spectrometry and collected. The solvent was removed by lyophilization to provide Boc-HYNIC-HBP (178 mg, 36.7%) as white crystals. ^{1}H NMR (D_2O): δ 8.42 (1H, s), 8.33 (1H, d), 7.21 (1H, d), 3.43 (2H, t), 1.92–2.04 (4H, m), 1.47 (9H, s). ESI-MS calculated for $C_{15}H_{26}N_4O_{10}P_2$ (M- H)$^-$: m/z 483. Found: 483.

Boc-HYNIC-HBP (10.4 mg, 21.5 μmol) was stirred in a mixed solution of TFA (720 μL) and anisole (80 μL) for 10 min at room temperature. After removal of the solvent under a stream of N_2, the residue was washed with dry ether to produce [4-[(6-hydrazinopyridine-3-carbonyl)amino]-1-hydroxy-1-phosphonobutyl]phosphonic acid (HYNIC-HBP) quantitatively as white crystals. ^{1}H NMR (D_2O): δ 8.33 (1H, s), 8.13 (1H, d), 7.01 (1H, d), 3.42 (2H, t), 1.94–2.04 (4H, m). ESI-MS calculated for $C_{10}H_{18}N_4O_8P_2$ (M- H)$^-$: m/z 383. Found: 383.

Forty microliters of HYNIC-HBP solution (3.75 mg/mL in 0.1 mol/L borate buffer, pH 9.5) were mixed successively with 200 μL of tricine solution (30 mg/mL in 10 mmol/L citrate buffer, pH 5.2), 200 μL of 3-acetylpyridine solution (10 μL/mL in 10 mmol/L citrate buffer, pH 5.2), 200 μL of $^{99m}TcO_4^-$ solution, and 25 μL of $SnCl_2$ solution (1.0 mg/mL in 0.1N HCl). The reaction mixture was vigorously stirred and allowed to react at 95°C for 35 min. ^{99m}Tc-HYNIC-HBP was purified by RP-HPLC under the same conditions as for the preparation of ^{99m}Tc-MAG3-HBP.

Hydroxyapatite-Binding Assay

The hydroxyapatite-binding assay was performed according to procedures described preciously with a slight modification (*14–16*). In brief, hydroxyapatite beads (Bio-Gel; Bio-Rad) were suspended in Tris/HCl-buffered saline (50 mmol/L, pH 7.4) at 1,

2.5, and 10 mg/mL. For the solutions of ^{99m}Tc-labeled compounds (^{99m}Tc-MAG3-HBP, ^{99m}Tc-HYNIC-HBP, and ^{99m}Tc-HMDP), the bisphosphonate concentrations were adjusted to 0.60 μmol/L. One hundred microliters of each solution of ^{99m}Tc-labeled compound were added to 100 μL of the hydroxyapatite suspension, and samples were gently shaken for 1 h at room temperature because it has been reported that 1 h was enough to attain binding equilibrium (*14*). After centrifugation at 10,000*g* for 5 min, the radioactivity of the supernatant was measured with an auto well γ-counter (ARC-2000; Aloka). Control experiments were performed with a similar procedure in the absence of hydroxyapatite beads. The rate of binding was determined as follows:

Hydroxyapatite binding (%) = (1 − [radioactivity of supernatant of each sample]/[radioactivity of supernatant in the respective control]) × 100.

Biodistribution Experiments

Animal experiments were conducted in accordance with our institutional guidelines, and the experimental procedures were approved by the Kyoto University Animal Care Committee. Biodistribution experiments were performed with an intravenous administration of 250 μL of each diluted tracer solution (370–740 kBq) to male Wistar rats (200–230 g). Groups of at least 4 rats each were sacrificed by decapitation at 5, 10, 30, and 60 min after injection. Organs of interest were removed and weighed, and radioactivity counts were determined with an auto well γ-counter and corrected for background radiation and physical decay during counting.

Serum Protein-Binding Assay

The binding of ^{99m}Tc-labeled compounds to serum protein was evaluated by ultrafiltration. Male Wistar rats (200–230 g) received a bolus of ^{99m}Tc-labeled compound by intravenous injection. At 3 min after the injection, the rats were anesthetized with ether and blood was collected by heart puncture. Each serum sample was prepared and applied to Centrifree units (Millipore). The units were centrifuged at 1,000*g* at room temperature. The radioactivity counts of the initial samples and filtrates were determined with an auto well γ-counter.

Statistical Analysis

Data are expressed as means ± SD where appropriate. Results of biodistribution experiments were statistically analyzed using a 1-way ANOVA followed by the Dunnett post hoc test. Differences were considered statistically significant when P values were less than 0.05.

RESULTS

Preparation of ^{99m}Tc-Labeled Compounds

^{99m}Tc-MAG3-HBP was prepared by complexation with ^{99m}Tc using $SnCl_2$ as a reductant. The radiochemical yield of ^{99m}Tc-MAG3-HBP was 73%. After purification by RP-HPLC, ^{99m}Tc-MAG3-HBP had a radiochemical purity of >95%.

HYNIC-HBP, the precursor of ^{99m}Tc-HYNIC-HBP, was synthesized by the coupling of the carboxyl group of Boc-HYNIC with the amino group of the bisphosphonate derivative and the subsequent deprotection of the Boc group. ^{99m}Tc-HYNIC-HBP was prepared by a 1-pot reaction of HYNIC-HBP with $^{99m}TcO_4^-$, tricine, and 3-acetylpyridine in the presence of $SnCl_2$. The radiochemical yield of ^{99m}Tc-HYNIC-HBP was 39%. After purification by RP-HPLC, ^{99m}Tc-HYNIC-HBP had a radiochemical purity of >95%.

Hydroxyapatite-Binding Assay

Figure 2 shows the percentage of each ^{99m}Tc-labeled compound bound to hydroxyapatite beads. With an increase in the amount of hydroxyapatite, the rate of binding rose. Both ^{99m}Tc-chelate−comjugated bisphosphonates (^{99m}Tc-MAG3-HBP and ^{99m}Tc-HYNIC-HBP) showed a significantly higher rate of binding than ^{99m}Tc-HMDP.

Biodistribution Experiments

The biodistributions of ^{99m}Tc-MAG3-HBP, ^{99m}Tc-HYNIC-HBP, and ^{99m}Tc-HMDP in normal rats are presented in Tables 1, 2, and 3. All ^{99m}Tc-labeled compounds accumulated rapidly and resided a long time in the femur. ^{99m}Tc-Chelate−conjugated bisphosphonates, ^{99m}Tc-MAG3-HBP and ^{99m}Tc-HYNIC-HBP, accumulated in bone in significantly larger amounts than ^{99m}Tc-HMDP. However, the bone-to-blood ratio of ^{99m}Tc-MAG3-HBP was decreased because its clearance from blood was delayed compared with that of ^{99m}Tc-HMDP. ^{99m}Tc-HYNIC-HBP had a significantly higher bone-to-blood ratio than ^{99m}Tc-HMDP because its clearance was equivalent to that of ^{99m}Tc-HMDP.

Serum Protein-Binding Assay

The proportions of ^{99m}Tc-MAG3-HBP and ^{99m}Tc-HYNIC-HBP bound to serum protein were 97.7% ± 0.2% and 88.7% ± 2.7%, respectively.

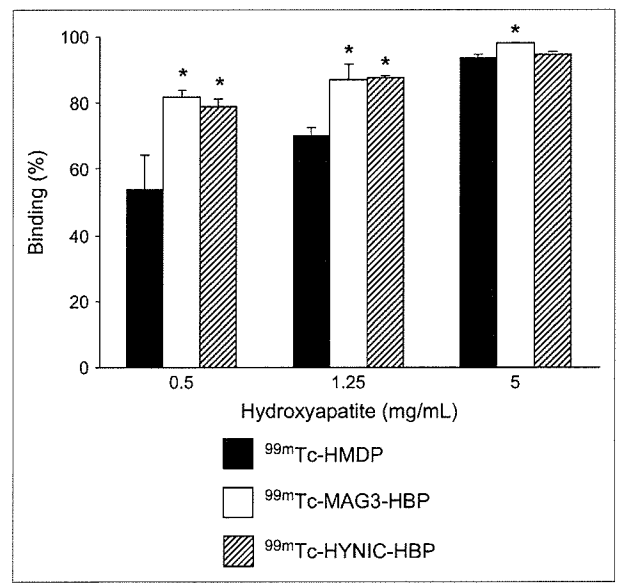

FIGURE 2. Binding of hydroxyapatite to ^{99m}Tc-MAG3-HBP, ^{99m}Tc-HYNIC-HBP, and ^{99m}Tc-HMDP. Data are expressed as mean ± SD for 3 or 4 experiments. Asterisks indicate statistically significant differences compared with ^{99m}Tc-HMDP with the Dunnett test ($P < 0.05$).

TABLE 1
Biodistribution of Radioactivity After Intravenous Administration of ^{99m}Tc-MAG3-HBP in Rats

Tissue	Time after administration (min)			
	5	10	30	60
Blood	0.98 ± 0.09*	0.77 ± 0.06	0.29 ± 0.01	0.07 ± 0.01*
Liver	0.32 ± 0.00	0.29 ± 0.03	0.18 ± 0.01	0.11 ± 0.02
Kidney	2.15 ± 0.33	1.87 ± 0.40	0.85 ± 0.05*	0.50 ± 0.08*
Intestine	0.16 ± 0.03*	0.15 ± 0.03*	0.13 ± 0.01*	0.17 ± 0.03*
Femur	1.80 ± 0.24	2.31 ± 0.22	3.73 ± 0.18*	4.23 ± 0.25*
F/B ratio†	1.86 ± 0.38*	3.02 ± 0.21*	13.1 ± 0.85*	59.7 ± 10.41

*Significant differences ($P < 0.05$) from ^{99m}Tc-HMDP were identified with the Dunnett test.
†Femur-to-blood ratio.
Each value is mean ± SD for 4 animals.

DISCUSSION

Radiopharmaceuticals with greater affinity for bone are expected to be effective in shortening the time interval between injection and bone imaging. Thus, based on the concept of bifunctional radiopharmaceuticals, ^{99m}Tc-chelate–conjugated bisphosphonates were designed in this study. First, MAG3 was chosen as a ^{99m}Tc-chelating group because this N_3S ligand forms a relatively compact, hydrophilic, and stable complex with ^{99m}Tc in high yields (*17*). As expected, ^{99m}Tc-MAG3-HBP bound to the hydroxyapatite beads in vitro and accumulated in the rat femur in vivo to a greater extent than ^{99m}Tc-HMDP. However, the level of ^{99m}Tc-MAG3-HBP in blood was higher than that of ^{99m}Tc-HMDP, which resulted in a decreased bone-to-blood ratio. We attribute this high radioactivity of ^{99m}Tc-MAG3-HBP in blood to the binding of serum proteins because the ^{99m}Tc-MAG3 complex shows strong binding to serum proteins (*18,19*). In fact, the level of binding of ^{99m}Tc-MAG3-HBP to protein was very high.

HYNIC is a representative bifunctional chelating agent used to prepare ^{99m}Tc-labeled proteins and peptides with tricine as a coligand (*10,20–22*). However, it has been reported that the complex [^{99m}Tc](HYNIC)(tricine)$_2$ is not stable and exists in multiple forms, and the pharmacokinetics could be affected by the exchange reaction between tricine and protein in the plasma and tissues (*22–24*). To solve these problems, Liu et al. used several pyridine derivatives as coligands to form ternary ligand complexes, [^{99m}Tc](HYNIC)(tricine)(pyridine derivative), with greater stability and fewer isomers (*25*). Furthermore, in a previous study, we showed that little binding to plasma protein was displayed by ^{99m}Tc-HYNIC-labeled polypeptides derivatized with this ternary ligand complex (*13*). Then, ^{99m}Tc-HYNIC-HBP in which [^{99m}Tc](HYNIC)(tricine)(3-acetylpyridine) was conjugated with a bisphosphonate derivative, was designed for high bone affinity and rapid washout from the blood.

The rate of binding of ^{99m}Tc-HYNIC-HBP to serum protein was significantly lower than that of ^{99m}Tc-MAG3-HBP. When these values were expressed as a nonprotein–binding rate, the value of ^{99m}Tc-HYNIC-HBP (11.3%) is about 5 times the value of ^{99m}Tc-MAG3-HBP (2.3%). The difference in the binding of the compound to the serum protein affects its blood clearance (*26–28*). In fact, the blood clearance of ^{99m}Tc-HYNIC-HBP was significantly faster than that of ^{99m}Tc-MAG3-HBP and was equivalent to that

TABLE 2
Biodistribution of Radioactivity After Intravenous Administration of ^{99m}Tc-HYNIC-HBP in Rats

Tissue	Time after administration (min)			
	5	10	30	60
Blood	0.56 ± 0.05	0.39 ± 0.04*	0.10 ± 0.01	0.03 ± 0.01
Liver	0.18 ± 0.02	0.12 ± 0.01*	0.07 ± 0.01*	0.05 ± 0.01
Kidney	3.19 ± 1.02	1.43 ± 0.09	0.45 ± 0.05	0.26 ± 0.10
Intestine	0.15 ± 0.01*	0.10 ± 0.01	0.10 ± 0.07	0.05 ± 0.02
Femur	1.90 ± 0.21*	2.59 ± 0.22*	3.71 ± 0.30*	3.96 ± 0.36*
F/B ratio†	3.40 ± 0.50*	6.69 ± 0.43	37.1 ± 4.01*	123.20 ± 18.30*

*Significant differences ($P < 0.05$) from ^{99m}Tc-HMDP were identified with the Dunnett test.
†Femur-to-blood ratio.
Each value is mean ± SD for 6 animals.

TABLE 3
Biodistribution of Radioactivity After Intravenous Administration of ^{99m}Tc-HMDP in Rats

Tissue	Time after administration (min)			
	5	10	30	60
Blood	0.61 ± 0.03	0.32 ± 0.04	0.10 ± 0.01	0.04 ± 0.01
Liver	0.15 ± 0.02	0.08 ± 0.01	0.03 ± 0.00	0.04 ± 0.05
Kidney	3.11 ± 0.23	1.59 ± 0.42	0.46 ± 0.08	0.24 ± 0.03
Intestine	0.12 ± 0.00	0.09± 0.02	0.04 ± 0.01	0.03 ± 0.01
Femur	1.52 ± 0.14	1.97 ± 0.18	2.73 ± 0.15	3.16 ± 0.51
F/B ratio*	2.49 ± 0.15	6.27 ± 0.94	29.16 ± 4.86	93.40 ± 19.81

*Femur-to-blood ratio.
Each value is mean ± SD for 4 or 5 animals.

of ^{99m}Tc-HMDP, although factors other than protein binding may also be responsible for rapid blood clearance. Furthermore, ^{99m}Tc-HYNIC-HBP accumulated in larger amounts in femur than did ^{99m}Tc-HMDP, which could be attributable to its design based on the bifunctional radiopharmaceutical concept. Consequently, the bone-to-blood ratio of ^{99m}Tc-HYNIC-HBP was significantly higher than that of ^{99m}Tc-HMDP.

We assume that ^{99m}Tc-chelate–conjugated bisphosphonates in bone remain intact because their ^{99m}Tc complexes are stable. On the other hand, previous studies suggested that there was a separation of the ^{99m}Tc-bisphosphonate complex into its ^{99m}Tc and bisphosphonate components before incorporation into the mineral phase (*29,30*). However, the separation of ^{99m}Tc-bisphosphonate must occur at the bone site because reduced ^{99m}Tc alone was not taken up by bone (*30*). Namely, there is little difference from the point of view that bisphosphonate is used as a carrier to bone in both cases. Thus, we hypothesized that the affinity of bisphosphonate for hydroxyapatite is important for bone accumulation and it would be increased by the design of a bisphosphonate in which the phosphonate groups do not coordinate with technetium. In fact, ^{99m}Tc-chelate–conjugated bisphosphonates had better affinity for hydroxyapatite and accumulated in the rat femur in vivo to greater extent than ^{99m}Tc-HMDP. These results support our hypothesis. However, other factors such as the blood circulation and delivery of the agents may also be important. Further study may be required to elucidate the mechanism for bone localization.

Because MAG3-HBP and HYNIC-HBP contain a bisphosphonate site, there is the possibility that ^{99m}Tc coordinates not with the MAG3 moiety or the HYNIC moiety but rather with the bisphosphonate moiety. To ascertain that ^{99m}Tc is chelated with only the MAG3 moiety, Re-MAG3-HBP was prepared by the coupling of nonradioactive Re-MAG3 complexed previously with the bisphosphonate analog. By RP-HPLC analysis, identical retention times between ^{99m}Tc-MAG3-HBP and Re-MAG3-HBP were exhibited (Fig. 3), revealing their structural analogy. In the case of the HYNIC complex, because it is difficult to synthesize the corresponding stable Re-HYNIC complex, ^{99m}Tc-HYNIC-HBP was prepared by the coupling of [^{99m}Tc](HYNIC-TFP)(tricine)(3-acetylpyridine) with the bisphosphonate derivative. RP-HPLC analysis revealed this ^{99m}Tc-labeled product to be identical to that obtained from the reaction of HYNIC-HBP with $^{99m}TcO_4^-$, tricine, and 3-acetylpyridine in the presence of $SnCl_2$ (Fig. 4). These findings exclude the possibility of complexation between technetium and the bisphosphonate structure and indicate the chelation of ^{99m}Tc with only the MAG3 moiety in MAG3-HBP and the HYNIC moiety in HYNIC-HBP.

CONCLUSION

As a radiopharmaceutical that accumulates at high level in bone and is rapidly cleared from blood, we designed a novel ^{99m}Tc-chelate–conjugated bisphosphonate, ^{99m}Tc-HYNIC-HBP. ^{99m}Tc-HYNIC-HBP had good affinity for hydroxyapatite crystals and showed lower binding to serum proteins. In rat biodistribution experiments, ^{99m}Tc-HYNIC-HBP had a higher bone-to-blood accumulation ratio of radioactivity at early times after injection than ^{99m}Tc-HMDP.

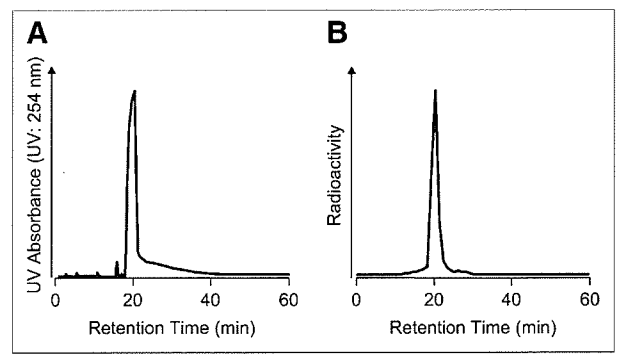

FIGURE 3. RP-HPLC chromatograms of nonradioactive Re-MAG3-HBP (A) and ^{99m}Tc-MAG3-HBP (B). Conditions: flow rate of 1 mL/min with 10% ethanol in 200 mmol/L phosphate buffer (pH 6.0) containing 10 mmol/L tetrabutylammoniumhydroxide.

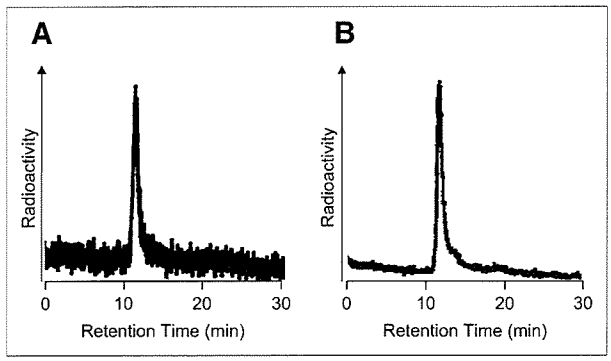

FIGURE 4. RP-HPLC chromatograms of ^{99m}Tc-HYNIC-HBP prepared by coupling of [^{99m}Tc](HYNIC-TFP)(tricine)(3-acetylpyridine) with bisphosphonate derivative (A) and labeling of HYNIC-HBP with $^{99m}TcO_4^-$, tricine, and 3-acetylpyridine (B). Conditions: flow rate of 1 mL/min with 10% ethanol in 200 mmol/L phosphate buffer (pH 6.0) containing 10 mmol/L tetrabutylammoniumhydroxide.

These results indicate that ^{99m}Tc-HYNIC-HBP holds great potential for bone scintigraphy.

ACKNOWLEDGMENTS

This work was supported in part by a Grant-in-Aid for Scientific Research from the Ministry of Education, Culture, Sports, Science and Technology of Japan and a research grant from the Sagawa Foundation for Promotion of Cancer Research.

REFERENCES

1. Subramanian G, McAfee JG, Blair RJ, Kallfelz FA, Thomas FD. Technetium-99m-methylene diphosphonate: a superior agent for skeletal imaging—comparison with other technetium complexes. *J Nucl Med.* 1975;16:744–755.
2. Domstad PA, Coupal JJ, Kim EE, Blake JS, DeLand FH. ^{99m}Tc-Hydroxymethane diphosphonate: a new bone imaging agent with a low tin content. *Radiology.* 1980;136:209–211.
3. Love C, Din AS, Tomas MB, Kalapparambath TP, Palestro CJ. Radionuclide bone imaging: an illustrative review. *Radiographics.* 2003;23:341–358.
4. Mari C, Catafau A, Carrio I. Bone scintigraphy and metabolic disorders. *Q J Nucl Med.* 1999;43:259–267.
5. Meyer JL, Nancollas GH. The influence of multidentate organic phosphonates on the crystal growth of hydroxyapatite. *Calcif Tissue Res.* 1973;13:295–303.
6. Libson K, Deutsch E, Barnett BL. Structural characterization of a technetium-99-diphosphonate complex: implications for the chemistry of technetium-99m skeletal imaging agents. *J Am Chem Soc.* 1980;102:2476–2478.
7. Hnatowich DJ, Qu T, Chang F, Ley AC, Ladner RC, Rusckowski M. Labeling peptides with technetium-99m using a bifunctional chelator of a N-hydroxysuccinimide ester of mercaptoacetyltriglycine. *J Nucl Med.* 1998;39:56–64.
8. Liu S, Edwards DS, Barrett JA. ^{99m}Tc labeling of highly potent small peptides. *Bioconjug Chem.* 1997;8:621–636.
9. Abrams MJ, Juweid M, tenKate CI, et al. Technetium-99m-human polyclonal IgG radiolabeled via the hydrazino nicotinamide derivative for imaging focal sites of infection in rats. *J Nucl Med.* 1990;31:2022–2028.
10. Ohtsuki K, Akashi K, Aoka Y, et al. Technetium-99m HYNIC-annexin V: a potential radiopharmaceutical for the in-vivo detection of apoptosis. *Eur J Nucl Med.* 1999;26:1251–1258.
11. Steffens MG, Oosterwijk E, Kranenborg MH, et al. In vivo and in vitro characterizations of three ^{99m}Tc-labeled monoclonal antibody G250 preparations. *J Nucl Med.* 1999;40:829–836.
12. Ogawa K, Mukai T, Arano Y, et al. Development of a rhenium-186-labeled MAG3-conjugated bisphosphonate for the palliation of metastatic bone pain based on the concept of bifunctional radiopharmaceuticals. *Bioconjug Chem.* 2005;16:751–757.
13. Ono M, Arano Y, Mukai T, et al. ^{99m}Tc-HYNIC-derivatized ternary ligand complexes for ^{99m}Tc-labeled polypeptides with low in vivo protein binding. *Nucl Med Biol.* 2001;28:215–224.
14. Fujisawa R, Kuboki Y. Preferential adsorption of dentin and bone acidic proteins on the (100) face of hydroxyapatite crystals. *Biochim Biophys Acta.* 1991;1075:56–60.
15. Kasugai S, Fujisawa R, Waki Y, Miyamoto K, Ohya K. Selective drug delivery system to bone: small peptide $(Asp)_6$ conjugation. *J Bone Miner Res.* 2000;15:936–943.
16. Ogawa K, Mukai T, Arano Y, et al. Rhemium-186-monoaminemonoamidedithiol-conjugated bisphosphonate derivatives for bone pain palliation. *Nucl Med Biol.* 2006;33:513–520.
17. Fritzberg AR, Kasina S, Eshima D, Johnson DL. Synthesis and biological evaluation of technetium-99m MAG3 as a hippuran replacement. *J Nucl Med.* 1986;27:111–116.
18. Verbruggen AM, Nosco DL, Van Nerom CG, Bormans GM, Adriaens PJ, De Roo MJ. Technetium-99m-L,L-ethylenedicysteine: a renal imaging agent. I. Labeling and evaluation in animals. *J Nucl Med.* 1992;33:551–557.
19. Taylor A Jr, Eshima D, Christian PE, Wooten WW, Hansen L, McElvany K. Technetium-99m MAG3 kit formulation: preliminary results in normal volunteers and patients with renal failure. *J Nucl Med.* 1988;29:616–622.
20. Verbeke K, Hjelstuen O, Debrock E, Cleynhens B, De Roo M, Verbruggen A. Comparative evaluation of $^{99}Tc^m$-Hynic-HSA and $^{99}Tc^m$-MAG3-HSA as possible blood pool agents. *Nucl Med Commun.* 1995;16:942–957.
21. Van der Laken CJ, Boerman OC, Oyen WJG, et al. Technetium-99m-labeled chemotactic peptides in acute infection and sterile inflammation. *J Nucl Med.* 1997;38:1310–1315.
22. Liu S, Edwards DS, Looby RJ, et al. Labeling a hydrazino nicotinamide-modified cyclic IIb/IIIa receptor antagonist with ^{99m}Tc using aminocarboxylates as coligands. *Bioconjug Chem.* 1996;7:63–71.
23. Ono M, Arano Y, Uehara T, et al. Intracellular metabolic fate of radioactivity after injection of technetium-99m-labeled hydrazino nicotinamide derivatized proteins. *Bioconjug Chem.* 1999;10:386–394.
24. Ono M, Arano Y, Mukai T, et al. Plasma protein binding of ^{99m}Tc-labeled hydrazino nicotinamide derivatized polypeptides and peptides. *Nucl Med Biol.* 2001;28:155–164.
25. Liu S, Edwards DS, Harris AR. A novel ternary ligand system for ^{99m}Tc-labeling of hydrazino nicotinamide-modified biologically active molecules using imine-N-containing heterocycles as coligands. *Bioconjug Chem.* 1998;9:583–595.
26. Vallner JJ. Binding of drugs by albumin and plasma protein. *J Pharm Sci.* 1977;66:447–465.
27. Daneshmend TK, Warnock DW. Clinical pharmacokinetics of systemic antifungal drugs. *Clin Pharmacokinet.* 1983;8:17–42.
28. Ogiso T, Iwaki M, Konishi Y. Effect of furosemide on plasma clearance, anticoagulant effect and protein binding of warfarin in rats. *J Pharmacobiodyn.* 1982;5:829–840.
29. van Langevelde A, Driessen OMJ, Pauwels EKJ, Thesingh CW. Aspects of ^{99m}technetium binding from an ethane-1-hydroxy-1,1-diphosphonate ^{99m}Tc complex to bone. *Eur J Nucl Med.* 1977;2:47–51.
30. Schwartz Z, Shani J, Soskolne WA, Touma H, Amir D, Sela J. Uptake and biodistribution of technetium-99m-MD^{32}P during rat tibial bone repair. *J Nucl Med.* 1993;34:104–108.

Available online at www.sciencedirect.com

SCIENCE DIRECT®

Nuclear Medicine and Biology 33 (2006) 513–520

NUCLEAR MEDICINE — AND — BIOLOGY

www.elsevier.com/locate/nucmedbio

Rhemium-186-monoaminemonoamidedithiol-conjugated bisphosphonate derivatives for bone pain palliation

Kazuma Ogawa[a,b], Takahiro Mukai[a,c], Yasushi Arano[d], Akira Otaka[a], Masashi Ueda[a], Tomoya Uehara[d], Yasuhiro Magata[e], Kazuyuki Hashimoto[f], Hideo Saji[a,*]

[a]*Graduate School of Pharmaceutical Sciences, Kyoto University, Yoshida Shimoadachi-cho, Sakyo-ku, Kyoto 606-8501, Japan*
[b]*Advanced Science Research Center, Kanazawa University, Kanazawa 920-8640, Japan*
[c]*Graduate School of Pharmaceutical Sciences, Kyushu University, Higashi-ku, Fukuoka 812-8582, Japan*
[d]*Graduate School of Pharmaceutical Sciences, Chiba University, Chuo-ku, Chiba 260-8675, Japan*
[e]*Photon Medical Research Center, Hamamatsu University School of Medicine, Hamamatsu 431-3192, Japan*
[f]*Japan Atomic Energy Research Institute, Tokai-mura, Ibaraki 319-1195, Japan*

Received 14 October 2005; received in revised form 17 March 2006; accepted 17 March 2006

Abstract

To develop a radiopharmaceutical for the palliation of painful bone metastases based on the concept of bifunctional radiopharmaceuticals, we synthesized a bisphosphonate derivative labeled with rhenium-186 (^{186}Re) that contains a hydroxyl group at the central carbon of its bisphosphonate structure, we attached a stable ^{186}Re-MAMA chelate to the amino group of a 4-amino-butylidene-bisphosphonate derivative [*N*-[2-[[4-[(4-hydroxy-4,4-diphosphonobutyl)amino]-4-oxobutyl]-2-thioethylamino]acetyl]-2-aminoethanethiolate] oxorhenium (V) (^{186}Re-MAMA-HBP) and we investigated the effect of a hydroxyl group at the central carbon of its bisphosphonate structure on affinity for hydroxyapatite and on biodistribution by conducting a comparative study with [*N*-[2-[[3-(3,3-diphosphonopropylcarbamoyl)propyl]-2-thioethylamino]acetyl]-2-aminoethanethiolate] oxorhenium (V) (^{186}Re-MAMA-BP). The precursor of ^{186}Re-MAMA-HBP, trityl (Tr)-MAMA-HBP, was obtained by coupling a Tr-MAMA derivative to 4-amino-1-hydroxybutylidene-1,1-bisphosphonate. ^{186}Re-MAMA-HBP was prepared by a reaction with $^{186}ReO_4^-$ and $SnCl_2$ in citrate buffer after the deprotection of the Tr groups of Tr-MAMA-HBP. After reversed-phase high-performance liquid chromatography, ^{186}Re-MAMA-HBP had a radiochemical purity of over 95%. Compared with ^{186}Re-MAMA-BP, ^{186}Re-MAMA-HBP showed a greater affinity for hydroxyapatite beads in vitro and accumulated a significantly higher level in the femur in vivo. Thus, the introduction of a hydroxyl group into ^{186}Re complex-conjugated bisphosphonates would be effective in enhancing accumulation in bones. These findings provide useful information on the design of bone-seeking therapeutic radiopharmaceuticals.

Keywords: Rhenium-186; Monoaminemonoamidedithiols; Bisphosphonate; Bone; Palliation

1. Introduction

Many cancers, especially breast and prostate carcinomas, have a strong propensity to metastasize to the bone [1]. Bone metastases are usually associated with severe pain, which has an important impact on quality of life [2]. Standard treatment options for bone metastases include external beam radiotherapy [3], while internal radiotherapy with radiopharmaceuticals would be preferable if the patient has a large number of metastatic lesions [4,5].

Rhenium-186 (^{186}Re) is a useful radionuclide for internal radiotherapy. Thus, rhenium-186-1-hydroxyethylidene-1,1-diphosphonate (^{186}Re-HEDP) has been used for the palliation of metastatic bone pain [6-9]. However, ^{186}Re-HEDP showed delayed blood clearance and high gastric uptake of radioactivity upon injection [10]. These features were attributed to the generation of $^{186}ReO_4^-$ resulting from the instability of this ^{186}Re complex in vivo [11,12]. To improve the instability of ^{186}Re-HEDP based on the concept of bifunctional radiopharmaceuticals, we recently developed

* Corresponding author. Department of Patho-Functional Bioanalysis, Graduate School of Pharmaceutical Sciences, Kyoto University, Yoshida Shimoadachi-cho, Sakyo-ku, Kyoto 606-8501, Japan. Tel.: +81 75 753 4556; fax: +81 75 753 4568.
E-mail address: hsaji@pharm.kyoto-u.ac.jp (H. Saji).

0969-8051/$ – see front matter © 2006 Elsevier Inc. All rights reserved.
doi:10.1016/j.nucmedbio.2006.03.006

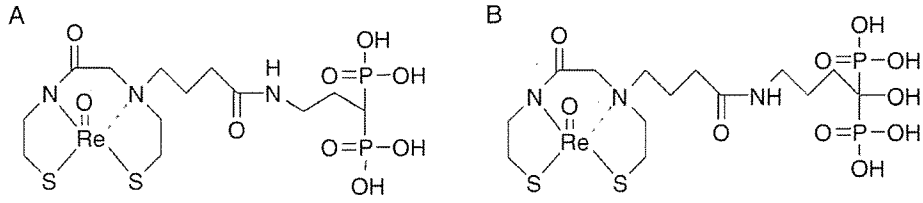

Fig. 1. Chemical structures of (A) Re-MAMA-BP and (B) Re-MAMA-HBP.

a new ^{186}Re-labeled bisphosphonate derivative through the conjugation of a stable ^{186}Re complex to a bisphosphonate analog [*N*-[2-[[3-(3,3-diphosphonopropylcarbamoyl)propyl]-2-thioethylamino]acetyl]-2-aminoethanethiolate] oxorhenium (V) (^{186}Re-MAMA-BP); Fig. 1A]. As expected, ^{186}Re-MAMA-BP was considerably more stable than ^{186}Re-HEDP in vitro [13].

Previous studies of bisphosphonates suggest that a hydroxyl group at a central carbon of the bisphosphonate structure affects the affinity for bone minerals [14,15]. Since extensive accumulation in bones is a definitive requirement for a therapeutic drug in the palliation of metastatic bone pain, we designed a ^{186}Re-MAMA-BP derivative with a hydroxyl group at a central carbon of the bisphosphonate structure, [*N*-[2-[[4-[(4-hydroxy-4,4-diphosphonobutyl)-amino]-4-oxobutyl]-2-thioethylamino]acetyl]-2-aminoethanethiolate]oxorhenium(V) **(6)** (^{186}Re-MAMA-HBP; Fig. 1B) in order to develop a ^{186}Re-labeled compound with greater accumulation in the bone. In this study, we synthesized ^{186}Re-MAMA-HBP and evaluated the effect of introducing a hydroxyl group at a central carbon of the bisphosphonate structure on the affinity for hydroxyapatite and on in vivo accumulation in the bone by studying and comparing it with ^{186}Re-HEDP and ^{186}Re-MAMA-BP.

2. Materials and methods

2.1. Materials

Ion spray mass spectrum was obtained with an API*III*E triple quadrupole mass spectrometer (Perkin-Elmer Science Instruments, Thornhill, Canada). Thin-layer chromatography (TLC) analyses were performed with silica plates (Silica Gel 60; Merck KGaA, Darmstadt, Germany), with acetone as developing solvent. ^{186}Re was supplied as $^{186}ReO_4^-$ by the Japan Atomic Energy Research Institute (Ibaraki, Japan) [16]. ^{186}Re-MAMA-BP and ^{186}Re-HEDP

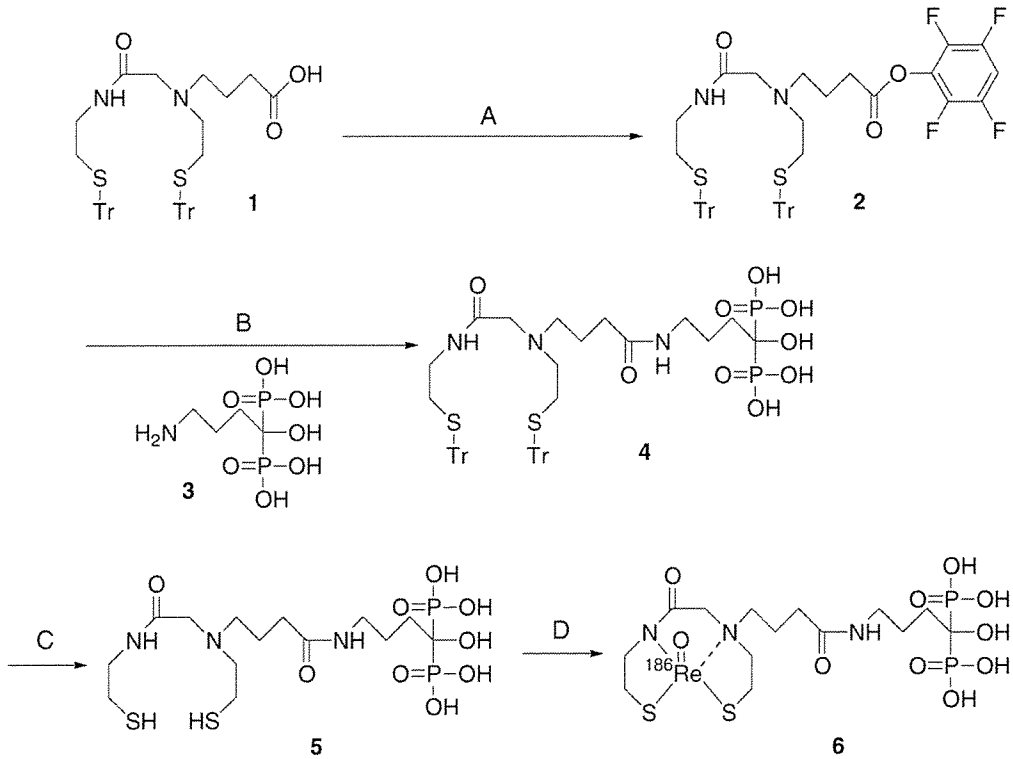

Scheme 1. Synthesis of ^{186}Re-MAMA-HBP. Reagents: (A) TFP and DCC; (B) Et_3N; (C) TFA and triethylsilane; (D) $^{186}ReO_4^-$ and $SnCl_2$/citrate.

were synthesized as described previously [13]. Other reagents were of reagent grade and were used as received.

2.2. Synthesis of ^{186}Re-MAMA-HBP

^{186}Re-MAMA-HBP was synthesized according to the procedure outlined in Scheme 1.

2.2.1. N^2-[4-[(4-hydroxy-4,4-diphosphonobutyl)amino]-4-oxobutyl]-N^1,N^2-bis[2-(tritylthio)ethyl]glycinamide [trityl (Tr)-MAMA-HBP] (4)

N-[2-(Tritylthio)ethylaminocarbonylmethyl]-*N*-[2-(tritylthio)ethyl]-4-aminobutyric acid **(1)** (172 mg, 0.225 mmol), synthesized as described previously [13], and tetrafluorophenol (TFP) (43.6 mg, 0.248 mmol) were dissolved in 3 ml of chloroform. Dicyclohexylcarbodiimide (DCC; 51.6 mg, 0.248 mmol) in 4 ml of chloroform was added dropwise to the reaction mixture at room temperature. After 1 h of stirring at room temperature, the solvent was removed in vacuo. The residue was then suspended in an adequate volume of ethyl acetate, DCC urea was removed by filtration and the filtrate was evaporated in vacuo to obtain crude [*N*-[2-(tritylthio)ethylaminocarbonylmethyl]-*N*-[2-(tritylthio)ethyl]-4-aminobutyric acid 2,3,5,6-tetrafluorophenyl ester (2). Compound **(2)** was used in the next reaction without further purification. 4-Amino-1-hydroxybutylidene-1,1-bisphosphonate **(3)** (57.0 mg, 0.229 mmol), synthesized according to the method of Kieczykowski [17], was suspended in 3 ml of distilled water, and triethylamine (140 mg, 1.39 mmol) was added to the suspension. After a few seconds of stirring at room temperature, the suspension became clear. Compound **(2)** was dissolved in 4 ml of acetonitrile and was then added to the reaction mixture. Triethylamine (23.3 mg, 231 μmol) was then added, and the reaction mixture was stirred for 3 h at room temperature. This mixture was purified by reversed-phase high-performance liquid chromatography (RP-HPLC), which was performed with a Cosmosil $5C_{18}$-AR-300 column (10× 150 mm; Nacalai Tesque, Kyoto, Japan) at a flow rate of 4.7 ml/min with a gradient mobile phase from 5% acetonitrile in water with 0.1% trifluoroacetic acid (TFA) to 100% acetonitrile with 0.1% TFA for 30 min. Chromatograms were obtained by monitoring ultraviolet adsorption at a wavelength of 254 nm. The fraction containing Tr-MAMA-HBP **(4)** was determined by mass spectrometry and then collected. The solvent was removed by lyophilization to provide Tr-MAMA-HBP **(4)** (66.0 mg, 29.5%) as white crystals [ion spray mass spectrum calculated for $C_{52}H_{59}N_3O_9P_2S_2$ $(M+H)^+$: *m/z* 996; found: 996].

2.2.2. ^{186}Re-MAMA-HBP (6)

The Tr groups of Tr-MAMA-HBP were deprotected just before radiolabeling. Tr-MAMA-HBP **(4)** (0.3 mg) was dissolved in 190 μL of TFA and 10 μL of triethylsilane and then gently shaken. After the removal of the solvent under a stream of N_2, 0.1 ml of 0.2 M acetate buffer (pH 3.0) was added to the residue. To this solution were added stannous chloride (0.3 mg) in 0.1 ml of 0.1 M citrate buffer (pH 5.0) and 0.1 ml of $^{186}ReO_4^-$ solution. The mixture was vigorously stirred and allowed to react at 90°C for 1 h. After cooling to room temperature, ^{186}Re-MAMA-HBP was purified by RP-HPLC (Cosmosil $5C_{18}$-AR-300 column, 4.6×150 mm) and eluted with a mixture of 0.2 M phosphate buffer (pH 6.0) and ethanol (85:15) containing 10 mM tetrabutylammonium hydroxide at a flow rate of 1 ml/min. Radiochemical purity was determined by RP-HPLC and TLC.

2.3. In vitro stability

To evaluate the stability of ^{186}Re-MAMA-HBP in vitro, ^{186}Re-MAMA-HBP was diluted with 0.1 M phosphate buffer (pH 7.0) saturated with 95% O_2/5% CO_2, and the solution was incubated at 37°C for 24 h. After 1, 3, 6 and 24 h of incubation, the samples were drawn, and radioactivity was analyzed by RP-HPLC and TLC.

2.4. Biodistribution experiments

Animal experiments were conducted in accordance with our institutional guidelines, and experimental procedures were approved by the Kyoto University Animal Care Committee. Biodistribution experiments were performed by the intravenous administration of ^{186}Re-labeled compounds to 6-week-old male ddY mice (27–30 g). Groups of five or six mice each were administered 100 μL of each ^{186}Re-labeled compound and sacrificed at 10 min, 1 h, 3 h, 6 h and 24 h postinjection. Tissues of interest were removed and weighed. The whole left femur was isolated as a representative bone sample. Radioactivity levels in these tissues were determined with an autowell gamma counter (ARC 2000; Aloka, Tokyo, Japan).

2.5. Hydroxyapatite binding assay

The binding assay was performed as described previously, with slight modifications [18,19]. In brief, hydroxyapatite beads (Bio-Gel; Bio-Rad, Hercules, CA) were suspended in Tris/HCl-buffered saline (50 mM, pH 7.4) at 1, 10 and 25 mg/ml. One hundred microliters of ^{186}Re-MAMA-HBP, ^{186}Re-MAMA-BP or ^{186}Re-HEDP was added to the suspension (100 μL), and the mixture was gently shaken for 1 h at room temperature. After centrifugation at 10,000×*g* for 5 min, the radioactivity of the supernatant was measured. Control experiments were performed with a similar procedure in the absence of hydroxyapatite beads. The binding ratios were determined as follows:

$$\text{Hydroxyapatite binding (\%)} = 1 - \frac{\text{radioactivity of the supernatant of each sample}}{\text{radioactivity of the supernatant in the respective control}} \times 100.$$

The effect of bisphosphonate on the binding of ^{186}Re-MAMA-HBP to hydroxyapatite beads was also examined.

Table 1
Stability of ^{186}Re-MAMA-HBP in buffered solution

Incubation period (h)	Radiochemical purity (%)	S.D.
0	97.95	0.33
1	98.50	0.65
3	97.55	1.17
6	94.91	0.27
24	75.55	1.57

Each value represents the mean (S.D.) for three experiments.

One hundred microliters of ^{186}Re-MAMA-HBP, which additionally contained a different amount of HEDP, was incubated with 100 μL of the suspension containing 1 mg of hydroxyapatite beads. After centrifugation, the radioactivity of the supernatant was measured.

2.6. Determination of the partition coefficient

The partition coefficients of ^{186}Re-labeled compounds were measured as follows: a 10-μL aliquot of ^{186}Re-labeled compound was mixed with 3 g each of 1-octanol and phosphate buffer (0.1 M, pH 7.4) in a test tube. The mixture was vortexed (3×1 min) then stood for 20 min. After the procedure had been repeated thrice, the mixture was centrifuged at 1000×*g* for 5 min. Two 1-ml aliquots of each phase were removed, and their radioactivity was measured with a well counter. The partition coefficient was determined by calculating the ratio of 1-octanol to the buffer and was expressed as a common logarithm (log PC).

2.7. Radiation dose estimates

Residence times were calculated by monoexponential extrapolation of biodistribution data. According to residence times, radiation doses were calculated for adult patients using the MIRDOSE 3.1 program.

2.8. Statistical analysis

Throughout this paper, data are expressed as mean±S.D. In biodistribution experiments, data were compared for each time point using the Tukey–Kramer test. In hydroxyapatite binding experiments, the binding rates of ^{186}Re-MAMA-BP and ^{186}Re-MAMA-HBP for each concentration of hydroxyapatite were compared using unpaired Student's *t* test. $P = .05$ was defined as the limit of significance.

3. Results

3.1. Preparation of ^{186}Re-MAMA-HBP

For the synthesis of the precursor of ^{186}Re-MAMA-BP, Tr-MAMA-BP, a bisphosphoric tetraethyl ester derivative was conjugated with compound **(1)** (Tr-MAMA derivative) in the presence of DCC. After the hydrolysis of tetraethyl esters, Tr-MAMA-BP was obtained in good yield [13]. However, for the synthesis of the ^{186}Re-MAMA-HBP precursor, Tr-MAMA-HBP, bisphosphoric tetraalkyl esters with a hydroxyl group at the central carbon could not be synthesized. Thus, a bisphosphonate derivative **(3)** that has no protecting

Table 2
Biodistribution of radioactivity after intravenous administration of ^{186}Re-MAMA-HBP, ^{186}Re-MAMA-BP and ^{186}Re-HEDP in mice

Tissue	Time after administration				
	10 min	1 h	3 h	6 h	24 h
^{186}Re-MAMA-HBP					
Blood[a]	3.15[b] (0.46)	0.27[b,c] (0.04)	0.12[b,c] (0.03)	0.07[c] (0.01)	0.02[c] (0.01)
Liver[a]	4.10[b,c] (0.60)	4.70[c] (0.62)	3.02[b,c] (0.64)	1.91[c] (0.68)	0.52[c] (0.12)
Kidneys[a]	9.28 (4.40)	3.54[b] (1.07)	3.80[c] (1.63)	3.26[c] (2.00)	0.87[b,c] (0.24)
Intestine[a]	0.76 (0.25)	1.04 (0.05)	1.52 (0.63)	2.14 (1.27)	0.13 (0.06)
Stomach[d]	0.69[c] (0.17)	0.53[c] (0.13)	0.54[c] (0.09)	0.42[c] (0.27)	0.36 (0.27)
Femur[a]	18.80[c] (3.59)	24.35[b,c](2.56)	25.25[b,c] (2.04)	22.74[c] (3.33)	24.80[c] (2.41)
^{186}Re-MAMA-BP					
Blood[a]	4.28[c] (0.38)	0.61 (0.19)	0.23[c] (0.04)	0.11[c] (0.04)	0.03 (0.01)
Liver[a]	5.66[c] (1.19)	4.19[c] (0.52)	2.25[c] (0.34)	1.31[c] (0.42)	0.71[c] (0.20)
Kidneys[a]	14.05[c] (3.51)	6.33[c] (2.06)	4.50[c] (0.53)	3.54[c] (0.73)	2.43[c] (0.53)
Intestine[a]	0.99 (0.18)	1.14 (0.12)	1.50 (0.09)	1.68 (1.52)	0.24 (0.14)
Stomach[d]	0.75 (0.25)	0.87[c] (0.26)	0.79[c] (0.15)	0.29[c] (0.08)	0.19 (0.04)
Femur[a]	16.41[c] (1.85)	20.07[c] (1.82)	19.78 (1.37)	20.86[c] (2.06)	21.38[c] (3.83)
^{186}Re-HEDP					
Blood[a]	2.70 (0.11)	0.62 (0.22)	0.41 (0.06)	0.27 (0.02)	0.04 (0.01)
Liver[a]	1.01 (0.16)	0.43 (0.22)	0.45 (0.15)	0.34 (0.10)	0.08 (0.01)
Kidneys[a]	7.92 (2.62)	2.24 (1.18)	1.37 (0.33)	1.02 (0.17)	0.42 (0.10)
Intestine[a]	0.64 (0.07)	0.92 (0.41)	1.34 (1.24)	2.13 (1.37)	0.37 (0.36)
Stomach[d]	1.26 (0.43)	2.72 (1.64)	2.54 (1.49)	1.17 (0.41)	0.57 (0.39)
Femur[a]	11.37 (1.23)	14.63 (2.60)	16.65 (3.16)	15.51 (4.00)	13.09 (2.90)

Each value represents the mean (S.D.) for five or six animals.
Significance was determined with the Tukey–Kramer test ($P<.05$).
[a] Expressed as percent injected dose per gram.
[b] Significantly different from ^{186}Re-MAMA-BP.
[c] Significantly different from ^{186}Re-HEDP.
[d] Expressed as percent injected dose.

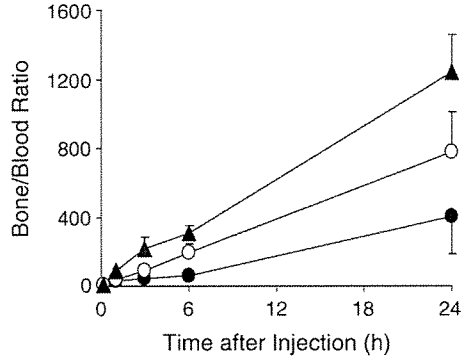

Fig. 2. Femur/blood ratios of radioactivity after the injection of ^{186}Re-MAMA-HBP (closed triangles), ^{186}Re-MAMA-BP (open circles) and ^{186}Re-HEDP (closed circles) in mice. Each value represents the mean± S.D. for five or six animals.

group was coupled with the active ester of the Tr-MAMA derivative **(2)**. Due to the insolubility of the bisphosphonate derivative **(3)** in organic solvents and the insolubility of the Tr-MAMA derivative **(2)** in aqueous solvents, the coupling reaction was performed in a solvent mixed with acetonitrile and water. However, the reaction did not proceed because the bisphosphonate derivative was deposited in the solvent during the mixing step. When triethylamine was added to the reaction mixture, the bisphosphonate derivative was soluble. This allowed the reaction to proceed. As a result, Tr-MAMA-HBP could be obtained. ^{186}Re-MAMA-HBP was prepared by complexation with ^{186}Re using citrate/$SnCl_2$ as a reducing system, just after the Tr groups of Tr-MAMA-HBP were deprotected by treatment with TFA and triethylsilane. The radiochemical yield of ^{186}Re-MAMA-HBP was 54%. After

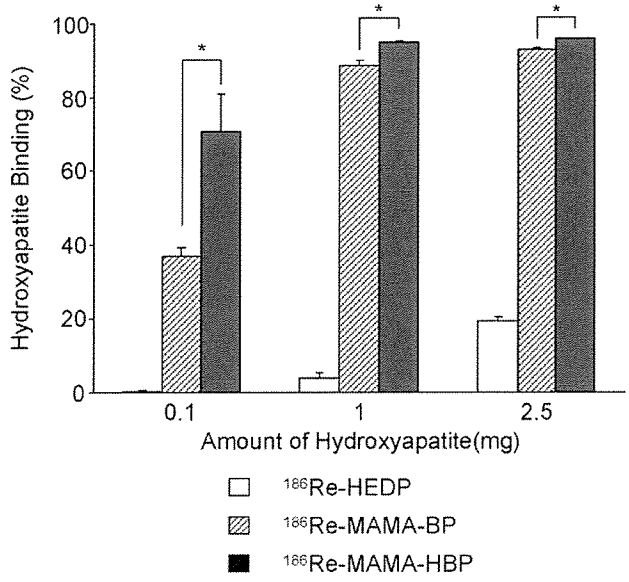

Fig. 3. Hydroxyapatite binding of ^{186}Re-labeled compounds. Each value represents the mean±S.D. for three samples. Significance was determined by unpaired Student's *t* test (*P<.05).

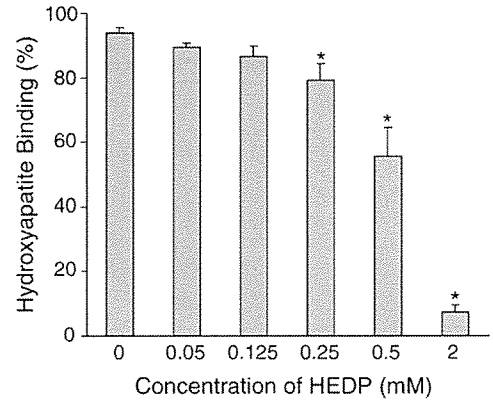

Fig. 4. Hydroxyapatite binding of ^{186}Re-MAMA-HBP and the inhibition of this binding by bisphosphonate (HEDP). Each value represents the mean±S.D. for three to six samples. The significance of differences was determined with a one-way analysis of variance followed by Dunnett's post hoc test, compared to samples without HEDP (*P<.05).

HPLC purification, ^{186}Re-MAMA-HBP had a radiochemical purity of over 95%. The radiochemical purity of both ^{186}Re-MAMA-BP and ^{186}Re-HEDP exceeded 95%.

3.2. In vitro stability

Table 1 shows the stability of ^{186}Re-MAMA-HBP in phosphate buffer. After 24 h of incubation, about 76% of ^{186}Re-MAMA-HBP remained intact. Under the same conditions, ^{186}Re-MAMA-BP showed stability similar to that of ^{186}Re-MAMA-HBP, whereas less than 30% of ^{186}Re-HEDP was intact [13].

3.3. Biodistribution experiments

The biodistribution of radioactivity after the intravenous injection of ^{186}Re-MAMA-HBP, ^{186}Re-MAMA-BP and ^{186}Re-HEDP in normal mice is summarized in Table 2. The tissue distribution of the radioactivity of ^{186}Re-MAMA-HBP was similar to that of ^{186}Re-MAMA-BP. ^{186}Re-MAMA-HBP, compared with ^{186}Re-MAMA-BP, showed a higher level in the femur and a faster blood clearance of radioactivity. Consequently, the femur/blood ratios of radioactivity were significantly higher after the administra-

Table 3
Absorbed dose estimates of ^{186}Re-MAMA-HBP, ^{186}Re-MAMA-BP and ^{186}Re-HEDP

Organ	^{186}Re-MAMA-HBP	^{186}Re-MAMA-BP	^{186}Re-HEDP
Bone surface[a]	6.13	5.71	2.02
Red marrow[a]	2.62	2.44	0.87
Liver[a]	0.08	0.09	0.01
Kidneys[a]	0.19	0.47	0.08
Small intestine[a]	0.10	0.08	0.10
Stomach[a]	0.09	0.05	0.14
Total body[a]	0.30	0.29	0.10
Effective dose[b]	0.46	0.42	0.19

[a] Expressed as milligrays per megabecquerel.
[b] Expressed as millisieverts per megabecquerel.

Table 4
Ratios of absorbed dose estimates between some organs and the bone surface

Organ	^{186}Re-MAMA-HBP	^{186}Re-MAMA-BP	^{186}Re-HEDP
Red marrow/ bone surface	0.427	0.427	0.431
Liver/ bone surface	0.013	0.016	0.005
Kidneys/ bone surface	0.031	0.082	0.040
Small intestine/ bone surface	0.016	0.014	0.050
Stomach/ bone surface	0.015	0.009	0.069
Total body/bone surface	0.049	0.051	0.050
Effective dose/ bone surface[a]	0.075	0.074	0.094

[a] Expressed as sieverts per gray.

tion of ^{186}Re-MAMA-HBP than after the administration of ^{186}Re-MAMA-BP (Fig. 2).

While ^{186}Re-HEDP also showed rapid accumulation and long retention in the femur, ^{186}Re-HEDP exhibited a significantly lower level of accumulation in the femur than ^{186}Re-MAMA-conjugated bisphosphonate derivatives (^{186}Re-MAMA-HBP and ^{186}Re-MAMA-BP). The blood clearance of ^{186}Re-HEDP was slower than that of ^{186}Re-MAMA-conjugated bisphosphonate derivatives. As a result, ^{186}Re-HEDP showed significantly lower femur/blood ratios of radioactivity (Fig. 2). Gastric accumulation of radioactivity after the administration of ^{186}Re-HEDP was higher, while hepatic and renal levels were lower than those of ^{186}Re-MAMA-conjugated bisphosphonate derivatives.

3.4. Hydroxyapatite binding assay

Fig. 3 shows the proportion of ^{186}Re-MAMA-BP, ^{186}Re-MAMA-HBP and ^{186}Re-HEDP that are bound to hydroxyapatite beads. With an increase in the amount of hydroxyapatite, the percentage of ^{186}Re-MAMA-BP, ^{186}Re-MAMA-HBP and ^{186}Re-HEDP that are bound to hydroxyapatite rose, and ^{186}Re-MAMA-HBP showed a significant increase compared with ^{186}Re-MAMA-BP. The binding affinity of ^{186}Re-HEDP to hydroxyapatite was much lower than that of ^{186}Re-MAMA-conjugated bisphosphonate, although strict comparison is difficult because of the difference in the concentrations of the ligand (bisphosphonate).

On the other hand, $^{186}ReO_4^-$ and ^{186}Re-MAMA hardly bound at all to hydroxyapatite beads (data not shown). The binding of ^{186}Re-MAMA-HBP was inhibited by the addition of a bisphosphonate compound (HEDP) in a concentration-dependent fashion (Fig. 4). These results indicated that the binding of ^{186}Re-MAMA-HBP to hydroxyapatite can be attributed to the character of the bisphosphonate site.

3.5. Partition coefficient

The log PC values of ^{186}Re-MAMA-BP and ^{186}Re-MAMA-HBP were much the same (-0.96 ± 0.01 vs. -1.02 ± 0.01), whereas ^{186}Re-HEDP had a lower log PC value (-1.54 ± 0.02).

3.6. Dosimetry

Table 3 shows absorbed radiation dose estimates for ^{186}Re-HEDP, ^{186}Re-MAMA-BP and ^{186}Re-MAMA-HBP. The radiation dose estimates for ^{186}Re-HEDP obtained in this study show similarity to those calculated from baboon data in van Aswegen et al. [20]. Table 4 shows the ratios of absorbed dose estimates between some organs and the bone surface. Since the bone surface is the target of internal radionuclide therapy, in obtaining an equal therapeutic effect, these ratios can be regarded as indices to unnecessary radiation. The red-marrow/bone-surface and total-body/bone-surface absorbed dose ratios are almost same among three compounds, and the effective-dose/bone-surface ratios of ^{186}Re-MAMA-BP and ^{186}Re-MAMA-HBP are lower than that of ^{186}Re-HEDP.

4. Discussion

The basic requirements for the effective use of radiopharmaceuticals in internal radiotherapy for the palliation of metastatic bone pain include extensive accumulation in the bone following peripheral administration.

Bisphosphonates have been used widely as inhibitors of bone resorption for the treatment of bone diseases and have been investigated extensively [21,22]. All bisphosphonates contain two phosphonate groups attached to a single carbon atom, forming a P–C–P structure; this central carbon has various side chains. Among these compounds, bisphosphonates containing a hydroxy group at the central carbon have been reported to have a higher affinity for bone minerals [14,15]. In addition, in the case of metal complexes, it was also reported that the cobalt (III) hydroxymethylene diphosphonate (HMDP) complex had a higher affinity for calcium than the cobalt (III) methylene diphosphonate (MDP) complex [23]. Furthermore, in the case of radiopharmaceuticals, it was also reported that ^{99m}Tc-HMDP, compared with ^{99m}Tc-MDP, demonstrated a higher uptake in bones [24,25]. Thus, based on the concept of bifunctional radiopharmaceuticals, we synthesized ^{186}Re-MAMA-HBP, a compound with a stable ^{186}Re-MAMA chelate moiety attached to a bisphosphonate derivative containing a hydroxy group at the central carbon. As expected, ^{186}Re-MAMA-HBP showed greater affinity for bone minerals (hydroxyapatite) compared with ^{186}Re-MAMA-BP, a bisphosphonate derivative without a hydroxy group at the central carbon (Fig. 3). This characteristic was reflected in its behavior in vivo. Namely, in biodistribution experiments, more ^{186}Re-MAMA-HBP than ^{186}Re-MAMA-BP accumulated in the femur (Table 2). These findings suggest that a hydroxyl group at the central carbon in the design of a ^{186}Re-chelate-conjugated bisphosphonate derivative is effective in enhancing accumulation in bones. Furthermore, ^{186}Re-MAMA-HBP showed higher accumulation in the femur, a

lower level in the stomach and more rapid clearance from the blood than ^{186}Re-HEDP (Table 2). These findings indicated high affinity for bone and good stability in vivo, reflecting the results of experiments in vitro (Fig. 3, Table 1). These results demonstrate that MAMA moiety is useful as a chelating group in forming a stable complex with ^{186}Re in a bifunctional radiopharmaceutical containing bisphosphonate as a biologically active molecule.

We expected that these results would lead to a decrease in the level of unnecessary radiation. Certainly, the radiation dose of ^{186}Re-MAMA-HBP for the stomach decreased, compared with ^{186}Re-HEDP. However, in the case of radiation dose for the bone marrow, known as the dose-limiting factor of bone-seeking agents, the absorbed dose ratio between the bone marrow and the bone surface of ^{186}Re-MAMA-HBP was equivalent to that of ^{186}Re-HEDP. The slight improvement of blood clearance should contribute little to the radiation dose for the bone marrow because the radiation dose for the bone marrow is highly influenced by the accumulation of radioactivity in the bone.

The radiation dose of ^{186}Re-MAMA-HBP for the liver increased, compared with ^{186}Re-HEDP, because hepatic radioactivity levels were significantly higher after the administration of ^{186}Re-MAMA-HBP than after the administration of ^{186}Re-HEDP. Since ^{186}Re-MAMA-HBP was more lipophilic than ^{186}Re-HEDP, as evident from the partition coefficient (1-octanol/phosphate buffer, pH 7.4), extensive hepatic uptake of ^{186}Re-MAMA-HBP may be caused by increase in lipophilicity.

When bone affinity is compared with those of other bone-seeking agents measured in different species, uptake value is expressed as percent dose per gram of tissue times body weight, in order to normalize the difference in the weight of animals. The corresponding value of ^{186}Re-MAMA-HBP in the femur 1 h after injection was 694%. ^{153}Sm-ethylene diamine tetramethylene phosphonate (EDTMP) was approved by the Food and Drug Administration for the treatment of painful bone metastases in 1997, and the uptake value was 707% (2 h in rats) [26]. Since the uptake value of ^{186}Re-MAMA-HBP is comparable to that of ^{153}Sm-EDTMP, it is expected that ^{186}Re-MAMA-HBP will be of clinical use from the point of view of bone uptake. However, the nonosseous tissue clearance of ^{186}Re-MAMA-HBP must not be rapid as that of ^{153}Sm-EDTMP because it was reported that ^{99m}Tc-MDP and ^{153}Sm-EDTMP showed no significant soft tissue uptake [27].

In conclusion, based on the idea of bifunctional radiopharmaceuticals, we developed a ^{186}Re complex-conjugated bisphosphonate derivative with a hydroxy group, ^{186}Re-MAMA-HBP. When administered to mice, ^{186}Re-MAMA-HBP showed greater affinity for bones and much higher femur/blood ratios of radioactivity than either ^{186}Re-HEDP or ^{186}Re-MAMA-BP. These findings should provide useful information on the drug design of bone-seeking therapeutic radiopharmaceuticals.

Acknowledgments

This work was supported, in part, by Grants-in-Aid for Scientific Research from the Ministry of Education, Culture, Sports, Science and Technology of Japan and a research grant from the Sagawa Foundation for the Promotion of Cancer Research.

References

[1] Yoneda T, Sasaki A, Mundy GR. Osteolytic bone metastasis in breast cancer. Breast Cancer Res Treat 1994;32:73–84.
[2] Mercadante S. Malignant bone pain: pathophysiology and treatment. Pain 1997;69:1–18.
[3] Uppelschoten JM, Wanders SL, de Jong JM. Single-dose radiotherapy (6 Gy): palliation in painful bone metastases. Radiother Oncol 1995;36:198–202.
[4] Pandit-Taskar N, Batraki M, Divgi CR. Radiopharmaceutical therapy for palliation of bone pain from osseous metastases. J Nucl Med 2004; 45:1358–65.
[5] McEwan AJ. Use of radionuclides for the palliation of bone metastases. Semin Radiat Oncol 2000;10:103–14.
[6] Elder RC, Yuan J, Helmer B, Pipes D, Deutsch K, Deutsch E. Studies of the structure and composition of rhenium-1,1-hydroxyethylidene-diphosphonate (HEDP) analogues of the radiotherapeutic agent (186)ReHEDP. Inorg Chem 1997;36:3055–63.
[7] Kolesnikov-Gauthier H, Carpentier P, Depreux P, Vennin P, Caty A, Sulman C. Evaluation of toxicity and efficacy of ^{186}Re-hydroxyethylidene diphosphonate in patients with painful bone metastases of prostate or breast cancer. J Nucl Med 2000;41:1689–94.
[8] Limouris GS, Shukla SK, Condi-Paphiti A, Gennatas C, Kouvaris I, Vitoratos N, et al. Palliative therapy using rhenium-186-HEDP in painful breast osseous metastases. Anticancer Res 1997;17: 1767–72.
[9] O'Sullivan JM, McCready VR, Flux G, Norman AR, Buffa FM, Chittenden S, et al. High activity rhenium-186 HEDP with autologous peripheral blood stem cell rescue: a phase I study in progressive hormone refractory prostate cancer metastatic to bone. Br J Cancer 2002;86:1715–20.
[10] De Winter F, Brans B, Van De Wiele C, Dierckx RA. Visualization of the stomach on rhenium-186 HEDP imaging after therapy for metastasized prostate carcinoma. Clin Nucl Med 1999;24:898–9.
[11] de Klerk JM, van Dijk A, van het Schip AD, Zonnenberg BA, van Rijk PP. Pharmacokinetics of rhenium-186 after administration of rhenium-186-HEDP to patients with bone metastases. J Nucl Med 1992;33:646–51.
[12] Arano Y, Ono M, Wakisaka K, Uezono T, Akizawa H, Motonari Y, et al. Synthesis and biodistribution studies of ^{186}Re complex of 1-hydroxyethylidene-1,1-diphosphonate for treatment of painful osseous metastases. Radioisotopes 1995;44:514–22.
[13] Ogawa K, Mukai T, Arano Y, Hanaoka H, Hashimoto K, Nishimura H, et al. Design of a radiopharmaceutical for the palliation of painful bone metastases: rhenium-186-labeled bisphosphonate derivative. J Label Cmpd Radiopharm 2004;47:753–61.
[14] Meyer JL, Nancollas GH. The influence of multidentate organic phosphonates on the crystal growth of hydroxyapatite. Calcif Tissue Res 1973;13:295–303.
[15] van Beek E, Hoekstra M, van de Ruit M, Lowik C, Papapoulos S. Structural requirements for bisphosphonate actions in vitro. J Bone Miner Res 1994;9:1875–82.
[16] Kobayashi K, Motoishi S, Terunuma K, Rauf AA, Hashimoto K. Production of $^{186/188}$Re and recovery of tungsten from spent ^{188}W/^{188}Re generator. Radiochemistry 2000;42:551–4.
[17] Kieczykowski GR. New process for preparing an antihypercalcemic agent. UK Patent GB 2248061A, 1992.

[18] Kasugai S, Fujisawa R, Waki Y, Miyamoto K, Ohya K. Selective drug delivery system to bone: small peptide $(Asp)_6$ conjugation. J Bone Miner Res 2000;15:936–43.

[19] Fujisawa R, Kuboki Y. Preferential adsorption of dentin and bone acidic proteins on the (100) face of hydroxyapatite crystals. Biochim Biophys Acta 1991;1075:56–60.

[20] van Aswegen A, Roodt A, Marais J, Botha JM, Naude H, Lotter MG, et al. Radiation dose estimates of ^{186}Re-hydroxyethylidene diphosphonate for palliation of metastatic osseous lesions: an animal model study. Nucl Med Commun 1997;18:582–8.

[21] Fleisch H. Bisphosphonates: mechanisms of action. Endocr Rev 1998;19:80–100.

[22] Rodan GA, Fleisch HA. Bisphosphonates: mechanisms of action. J Clin Invest 1996;97:2692–6.

[23] Jurisson SS, Benedict JJ, Elder RC, Whittle R, Deutsch E. Calcium affinity of coordinated diphosphonate ligands. Single-crystal structure of $[(en)_2Co(O_2P(OH)CH_2P(OH)O_2]ClO_4 \cdot H_2O$. Implications for the chemistry of technetium-99m-diphosphonate skeletal imaging agents. Inorg Chem 1983;22:1332–8.

[24] Subramanian G, McAfee JG, Thomas FD, Feld TA, Zapf-Longo C, Palladino E. New diphosphonate compounds for skeletal imaging: comparison with methylene diphosphonate. Radiology 1983;149: 823–8.

[25] Fogelman I, Pearson DW, Bessent RG, Tofe AJ, Francis MD. A comparison of skeletal uptakes of three diphosphonates by whole-body retention: concise communication. J Nucl Med 1981; 22:880–3.

[26] Goeckeler WF, Edwards B, Volkert WA, Holmes RA, Simon J, Wilson D. Skeletal localization of samarium-153 chelates: potential therapeutic bone agents. J Nucl Med 1987;28:495–504.

[27] Ketring AR. ^{153}Sm-EDTMP and ^{186}Re-HEDP as bone therapeutic radiopharmaceuticals. Int J Rad Appl Instrum B 1987;14:223–32.

Available online at www.sciencedirect.com
SCIENCE DIRECT
Nuclear Medicine and Biology 33 (2006) 489–494
NUCLEAR MEDICINE — AND — BIOLOGY
www.elsevier.com/locate/nucmedbio

Development of a ^{111}In-labeled peptide derivative targeting a chemokine receptor, CXCR4, for imaging tumors

Hirofumi Hanaoka[a,b], Takahiro Mukai[c,d], Hirokazu Tamamura[a,e], Tomohiko Mori[c], Seigo Ishino[a], Kazuma Ogawa[a], Yasuhiko Iida[b], Ryuichiro Doi[c], Nobutaka Fujii[a], Hideo Saji[a,*]

[a]*Graduate School of Pharmaceutical Sciences, Kyoto University, Yoshida Shimoadachi-cho, Sakyo-ku, Kyoto 606-8501, Japan*
[b]*Graduate School of Medicine, Gunma University, Showa-machi, Maebashi 371-8511, Japan*
[c]*Graduate School of Medicine, Kyoto University, Shogoin Kawahara-cho, Sakyo-ku, Kyoto 606-8507, Japan*
[d]*Graduate School of Pharmaceutical Sciences, Kyushu University, Maidashi, Higashi-ku, Fukuoka 812-8582, Japan*
[e]*Institute of Biomaterials and Bioengineering, Tokyo Medical and Dental University, Chiyoda-ku, Tokyo 101-0062, Japan*

Received 7 October 2005; received in revised form 12 January 2006; accepted 12 January 2006

Abstract

The chemokine receptor CXCR4 is highly expressed in tumor cells and plays an important role in tumor metastasis. The aim of this study was to develop a radiopharmaceutical for the imaging of CXCR4-expressing tumors in vivo. Based on structure–activity relationships, we designed a 14-residue peptidic CXCR4 inhibitor, Ac-TZ14011, as a precursor for radiolabeled peptides. For ^{111}In-labeling, diethylenetriaminepentaacetic acid (DTPA) was attached to the side chain of D-Lys^{8} which is distant from the residues indispensable for the antagonistic activity. In-DTPA-Ac-TZ14011 inhibited the binding of a natural ligand, stromal cell-derived factor-1α, to CXCR4 in a concentration-dependent manner with an IC_{50} of 7.9 nM (Ac-TZ14011: 1.2 nM). In biodistribution experiments, more ^{111}In-DTPA-Ac-TZ14011 accumulated in the CXCR4-expressing tumor than in blood or muscle. Furthermore, the tumor-to-blood and tumor-to-muscle ratios were significantly reduced by coinjection of Ac-TZ14011, indicating a CXCR4-mediated accumulation in tumor. These findings suggested that ^{111}In-DTPA-Ac-TZ14011 would be a potential agent for the imaging of CXCR4 expression in metastatic tumors in vivo.

Keywords: CXCR4; Peptide radiopharmaceutical; Indium-111; Metastatic tumor

1. Introduction

Chemokines are a family of small proteins (8–14 kDa) that chemoattract leukocytes by binding to cell surface receptors, chemokine receptors [1]. The chemokine receptor family, which belongs to a superfamily of seven transmembrane domain G-protein-coupled receptors, comprises 18 members [2]. In 1996, one member, CXCR4, was identified as a coreceptor for the entry of T-cell line-tropic HIV-1 [3]. Since then, this receptor has attracted considerable attention as a pathogenic factor or a therapeutic target for HIV infection. Recent studies indicated that CXCR4 and its ligand, stromal cell-derived factor-1 (SDF-1), play an important role also in tumor metastasis [4–8]. Müller et al. [4] reported that CXCR4 was highly expressed in breast cancer and SDF-1 was highly expressed in organs representing the first destinations of metastasis. Moreover, they demonstrated that neutralization with anti-CXCR4 monoclonal antibody significantly inhibited the metastasis of breast cancer cells in mice. Similar results were obtained in other types of cancer [5–8]. These findings suggest that CXCR4 is a potential target for the in vivo imaging of metastatic tumors.

We have previously demonstrated that a peptide with anti-HIV-1 activity, T22 ([Tyr^{5,12}, Lys^{7}]-polyphemusin II), is an inhibitor of CXCR4 that blocks the entry of T-cell line-tropic HIV-1 mediated by this receptor. T22 is an 18-residue peptide amide, which was previously found by us based on an analysis of the structure–activity relationships of self-defense peptides of horseshoe crabs, tachyplesin and polyphemusin [9,10]. On the basis of the structure of T22, we designed and synthesized several downsized analogs, 14-residue peptides [11,12]. Among them, T140 showed the greatest inhibitory effect on the binding of an anti-CXCR4 monoclonal antibody to CXCR4 and the strongest inhibitory

* Corresponding author. Tel.: +81 75 753 4556; fax: +81 75 753 4568.
E-mail address: hsaji@pharm.kyoto-u.ac.jp (H. Saji).

0969-8051/$ – see front matter © 2006 Elsevier Inc. All rights reserved.
doi:10.1016/j.nucmedbio.2006.01.006

activity against HIV-1 entry [12]. The aim of this study was to develop a radiolabeled T140 derivative as an imaging agent for metastatic tumors. Considering that the three residues on the restricted backbone (L-3-(2-naphthyl)alanine (Nal)[3], Tyr[5] and Arg[14]) and the single residue in the flexible region (Arg[2]) form the intrinsic pharmacophore of T140 [13–15], we designed a 14-residue peptidic inhibitor, Ac-TZ14011, as the precursor for radiolabeled peptides (Fig. 1). This precursor contains the above four residues which are necessary for the inhibitory activity against CXCR4. Furthermore, for site-selective conjugation of radiolabels, Ac-TZ14011 has a single amino group (D-Lys[8]), which is distant from the pharmacophore, and the carboxyl group of Arg[14] of Ac-TZ14011 is protected via amidation for stability in vivo [16,17].

^{111}In constitutes one of the most useful radionuclides for the radiolabeling of peptides for diagnostic applications in nuclear medicine. Diethylenetriaminepentaacetic acid (DTPA) is still an attractive chelating agent with which to prepare ^{111}In-labeled peptides since it provides ^{111}In-labeled peptides with highly specific activity. In addition, the development of a monoreactive DTPA derivative has provided an easy and efficient way to prepare DTPA-conjugated peptides [18,19]. In this study, DTPA-Ac-TZ14011 was prepared using a monoreactive DTPA derivative and coordinated with nonradioactive In or radioactive ^{111}In. Furthermore, the antagonistic activity of In-DTPA-Ac-TZ14011 and in vivo behavior of ^{111}In-DTPA-Ac-TZ14011 were investigated and the applicability of ^{111}In-DTPA-Ac-TZ14011 as a radiopharmaceutical for imaging tumors was evaluated.

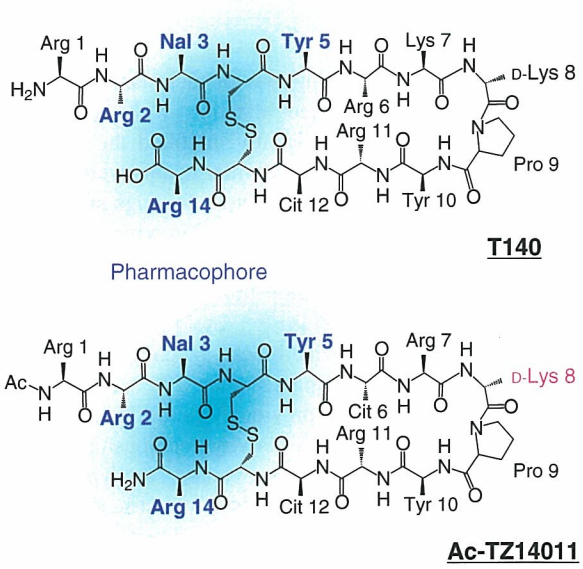

Fig. 1. Structures of T140 and Ac-TZ14011. There are four amino acid residues indispensable for the antagonistic activity (blue residues) which formed the pharmacophore. Nal: L-3-(2-naphthyl)alanine, Cit: L-citrulline. Ac-TZ14011 has a single amino group (D-Lys[8]) for site-selective conjugation of radiolabels, which is distant from the pharmacophore.

2. Materials and methods

2.1. Reagents and chemicals

$^{111}InCl_3$ (74 MBq/ml in 0.02N HCl) was kindly supplied by Nihon Medi-Physics (Nishinomiya, Japan). 9-Fluorenylmethoxycarbonyl (Fmoc)-protected amino acids and 4-(2′,4′-dimethoxyphenylaminomethyl)phenoxy (SAL) resin were purchased from Watanabe Chemical Industries (Hiroshima, Japan) or Calbiochem-Novabiochem Japan (Tokyo, Japan). 1-*tert*-Butyl hydrogen 3,6,9-tris((*tert*-butoxycarbonyl)methyl)-3,6,9-triazaundecanedioic acid (mDTPA) was synthesized as reported previously [18]. All the other chemicals were purchased from either Nacalai Tesque (Kyoto, Japan) or Wako Pure Chemical Industries (Osaka, Japan). Ion spray mass spectra (IS-MS) were obtained with the API III model (PerkinElmer Sciex Instruments, Thornhill, Canada). Cellulose acetate electrophoresis (CAE) strips were run in veronal buffer (pH 8.6, I=0.06) at a constant current of 0.8 mA for 40 min. Thin-layer chromatography (TLC) analyses were performed with silica plates (Silica gel 60, Merck, Darmstadt, Germany) with 10% aqueous ammonium chloride–methanol (1:1) as the developing solvent.

2.2. Synthesis of In-DTPA-Ac-TZ14011

Fig. 2 shows the scheme for the synthesis of In-DTPA-Ac-TZ14011. A protected peptide was constructed using Fmoc-based solid-phase synthesis on SAL resin and its N-terminus was acetylated. After being treated with thioanisole/trifluoroacetic acid (TFA) in the presence of *m*-cresol and 1,2-ethanedithiol, the crude peptide was air-oxidized and purified by reversed-phase HPLC (RP-HPLC). RP-HPLC was carried out with a Cosmosil 5C18-AR column (20×250 mm, Nacarai Tesque) eluted with a linear gradient of 10–30% acetonitrile in 0.1% aqueous TFA in 30 min at a flow rate of 7 ml/min. Fractions containing the peptide were collected, and the solvent was removed by lyophilization to afford Ac-TZ14011 as a white powder. IS-MS calcd for $C_{92}H_{144}N_{35}O_{19}S_2$ [M+H$^+$]: *m/z* 2107.1, found: *m/z* 2107.4.

DTPA-Ac-TZ14011 was prepared by mDTPA conjugation. Briefly, to a solution of mDTPA (19 mg, 30.8 μmol) in acetonitrile (350 μl) were added *N*-hydroxysuccinimide (3.74 mg, 32.3 μmol) and *N*,*N*-dicyclohexylcarbodiimide (6.67 mg, 32.3 μmol) at 0°C, and the mixture was incubated overnight at room temperature. After cooling to 0°C again, 200 μl of Ac-TZ14011 (10.2 mg, 3.65 μmol) in a mixture of acetonitrile and phosphate-buffered saline (pH 7.4) (1:1) was added to the reaction mixture and incubated overnight at room temperature. After treatment with 95% TFA, the crude peptide was purified by RP-HPLC under the same conditions as above. IS-MS calcd for $C_{106}H_{165}N_{38}O_{28}S_2$ [M+H$^+$]: *m/z* 2482.2, found: *m/z* 2482.9.

Fifty microliters of DTPA-Ac-TZ14011 (610 μg, 0.20 μmol) in 0.1 M acetic acid was reacted with 25 μl of nonradioactive $InCl_3 \cdot 4H_2O$ (64.5 μg, 0.22 μmol) in 0.02N HCl for 30 min at room temperature. Subsequent